Defects in resolution of inflammation: a hybrid model of neutrophil efferocytosis

Ed Long, CoMPLEX
Supervisors: Dr. Sylvia Nagl & Dr. Steven Barrett
Word Count: 12 161

August 31, 2007

Inflammation is an inherently paradoxical mechanism, vital for defence and repair in the face of microbial invasion and physical trauma but with the potential itself to cause damage to the host, sometimes leading to pathogenesis of chronic disorders. The fine balance regulating this operation relies on the complex interplay of a number of cell types and signalling molecules. In the human lung, alveolar macrophages play a central role in clearance of inflammatory cells as well as preventing their further influx.

This essay reviews experimental results relating to inflammatory cell clearance and uses a combination of mathematical and agent-based modelling techniques to perform an initial investigation into the dynamics of inflammatory cells and signalling molecules during the resolution phase of acute lung inflammation. The model predicts that lung collectins as well as impedance of cell movement within alveoli both have significant potential to instigate chronically inflamed states in comparison to variation in the expression of pro- or anti-inflammatory cytokines.

Contents

1 Introduction

In constructing models of complex biological systems, two popular methods of simulation are to use either an analytical or agent-based approach. Analytical models are essentially deterministic, rigorous and driven by differential equations. They are used to describe predator-prey population models in ecology; fluid flows in physiology or aerodynamics; diffusion dynamics in chemistry; and pharmacological applications such as PKPD[1] and ADME[2].

Agent-based modelling can be used to investigate systems that can be broken into populations of individual entities or *agents*. These typically follow rule-based behaviour based on local information which often gives rise to recognisable patterns at the population level which are not straightforward to predict from the local rules. This approach abstains from the often artificial 'designed dynamics' used in more traditional modelling paradigms, instead allowing the global-level patterns to emerge from the underlying mechanisms. In this manner, one can use global outcomes which differ markedly from observed behaviour to reject hypotheses on which the model is built in the manner of a computer-aided *Gedankenexperiment*.

While agent-based modelling has a relatively developed long history of application to ecological and social systems (where it is more commonly referred to as individual-based modelling, or IBM—see [1, 2]) it is now increasingly of interest in the field of biomedical research, particularly for investigating the dynamics of multi-cell systems.

Notable examples of this modelling paradigm include John Conway's *Game of Life* in which a rectangular grid is seeded with an initial pattern of 'live' cells and, in subsequent timesteps, cells determine whether they are live or dead according to the following rules:

1. A cell with fewer than live two neighbors is dead in the next timestep.
2. A cell with more than three live neighbors is dead in the next timestep from suffocation.
3. A live cell with two or three live neighbors stays alive in the next timestep.
4. A dead cell with exactly three live neighbors becomes alive in the next timestep.

In many 'seedings' of the grid the population of live cells quickly dies out but there exist certain initial configurations which support live cells over an extended period of time and feature a cluster of cells which appear to 'migrate' across the screen.

A second agent-based model worthy of mention is Craig Reynolds' technical Oscar-winning *Boids* algorithm which reproduces behaviour similar to the flocking of birds or schooling of fish: no single agent controls the movement of the group but local information based on the direction of surrounding agents, avoidance of nearby agents, momentum from the agents' current direction and a random component produces highly coherent mass movement for certain combinations of parameter values.

Cell populations are systems which are difficult to describe purely in terms of an analytic or behaviour-driven model. The large variety of specific behaviours and significance of position in relation to other cell-types make use of analytical models at the least unintuitive if not impossible. On the other hand, cell behaviour is driven by complex molecular dynamics and gene regulatory responses which are inadequately described by simple stochastically controlled behaviours.

In response to this, a currently expanding area of research is that of developing *hybrid* models which attempt to combine discrete or continuous mathematical models of the molecular processes (diffusion, receptor dynamics, gene regulation, ...) which govern cell behaviour with an agent-based implementation of the cells themselves. This sidesteps the computationally-intensive approach of modelling cell-surface receptors and ligands as individual agents and the associated

[1] PharmacoKinetic/PharmacoDynamic
[2] Absorption-Distribution-Metabolism-Excretion

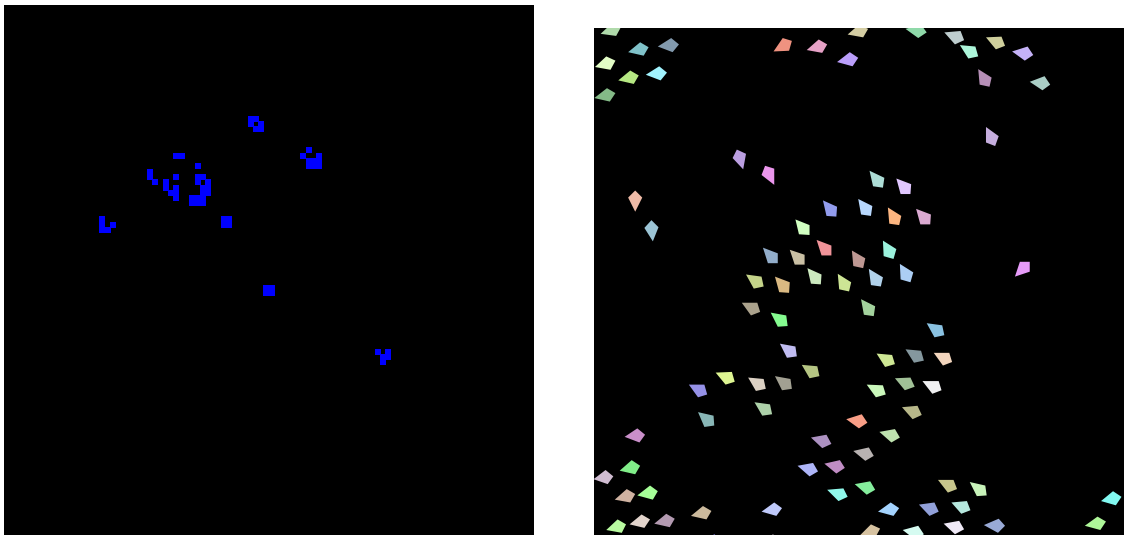

(a) (b)

Figure 1: Screenshots from Java implementations of the *Game of Life* and *Boids* simulations

worry of modelling agents at difference scales of time and space.

The 2006 paper of Dawn Walker *et al.* [3] describes extending their previous rule-based model *Epitheliome* to include epithelial growth factor receptor (EGFR) signalling between individuals in a population of epithelial cells. While behaviour of the cell agents was controlled by rules similar to those in the existing *Epitheliome* model, the signalling mechanics was mathematically modelled by a system of differential equations governing binding and dissociation of EGFR ligand, three-dimensional diffusion in the cell medium and the internalisation and trafficking of bound receptors. The mathematical component is then integrated with the behavioural component by allowing the receptor occupancy to affect the decision of cells whether to proliferate or become quiescent, though they note that the true system is more complex: receptor occupancy may also influence migration, differentiation, receptor repression and ligand release rates forming both positive and negative feedback loops. The group used this simulation to investigate the dependence of cell growth on the density of the cell population.

A second paper combining agent-based and mathematical methods to simulate cell behaviour is that of Christina Warrender *et al.* [4] (based on her 2004 thesis [5]). This paper concerns itself with survival and proliferation of alveolar macrophages in response to signalling via the signalling molecule macrophage colony stimulating factor (M-CSF). The approach was to test two alternative theories of the maintenance of macrophage population homeostasis: one where resident cells divide to replenish the population and one where resident cells assumed to be terminally differentiated (incapable of dividing), and it is cells entering the alveolus from the circulation which proliferate to maintain population numbers. While the simulation did not rule out either of the two mechanisms, it found the second was more stable under varying cell death and efflux rates.

While neither of these papers turn up any greatly unexpected property of the system under scrutiny, they offer methods for developing an integrated picture of a system at a greater level of detail than was previously possible. In terms of absolute predictive power, these models can only be as accurate as the data available to the developer but, even without aiming to perfectly reproduce the 'real system', implementing a few known agent-level behaviours within a realistic parameter space can strongly favour one hypothesis over another.

Griffin (2006) [6] and Bedau (1999) [7] gives accessible overviews on the process involved in developing agent-based models in theoretical biology and Thorne *et al.* (2007) [8] review a range of other papers dealing with the use of ABM in studying multi-cell interactions, also discussing the

nature of a model developer's relationship with traditional experimentalists. They conclude that the advance of biomedical research and its invariable increase in complexity necessitates the engagement of model developers and experimental teams. They further suggest that communication of cooperative efforts should be down two separate channels: publishing the abstract details of a model in a more theoretical journal and the comparison of the model findings with the experimental data in a life-sciences journal so that both sides can be fully explored and appropriately refereed.

This project also uses a mix of ABM and mathematical modelling techniques to investigate the interplay of immune cell signalling and behaviour within the lung. It deals with two cell types: both the alveolar macrophages studied in Warrender's paper and the smaller neutrophils, which migrate in large numbers to sites of inflammation. The model employs systems of interacting difference equations to drive cell signalling via pro- and anti-inflammatory cytokines.

2 Biological context

2.1 Background on inflammation

Inflammation as a defensive response to foreign elements is a vital and ancient ability, common to nearly all multicellular organisms[9]: recognition of the intruder, systemic signalling, recruitment of defensive agents and engulfment and lysis of the target is the sequence in an acute inflammatory response to a trigger such as bacterial infection or physical trauma. Recognition of this as an indicator of disease, likewise, has a long history in human civilisation: Egyptian heiroglyphics apparently demonstrate an awareness of its significance [10]. The Roman medical encyclopaedist Celsus is credited with first recording the four cardinal signs of acute inflammation: *rubor, calor, tumor* and *dolor* (respectively redness, heat, swelling and pain), to which *functio laesa* (loss of function) was added by the German doctor Rudolf Virchow in the 19th century.

The insight that inflammation is a defensive reaction of the body as opposed to an effect of disease is attributed to the Scottish surgeon John Hunter who wrote:

> "Inflammation in itself is not to be considered as a disease but as a salutary operation consequent to some violence or some disease[11]"

While this is true, extended periods of inflammation are not desirable: once an inflammatory response has reached its peak, the second phase—resolution—is also of great importance for the tissue to return to its homeostatic state. Both of these phases will be described in more detail below.

2.2 The acute response

The first line of defence against particles or microbes entering the body is typically a physical barrier—in the lungs this is provided by the mucociliary clearance system. This initial obstacle prevents the vast majority of invaders from reaching the epithelium of the lower respiratory tract. Those which are able to reach this point then trigger the intervention of the immune system. Local 'sentinel' immune effector cells (such as macrophages or dendritic cells) engage the foreign material and either deal with it themselves or, if the numbers are too great, release inflammatory mediators which recruit inflammatory cells from the bloodstream [12, 13]. Lambrecht [14] asserts that inactivated alveolar macrophages are still able to respond to small numbers of inhaled microorganisms (fewer than 10^9) without initiating expression of pro-inflammatory cytokines. When microbes present in larger numbers than this, there is a 'spillover' engaged by the dendritic cells which then present antigens, provoking signalling which attracts inflammatory leukocytes.

The most abundant of these is the neutrophil (the most common form of circulating *granulocyte*—along with eosinophils and basophils these are white blood cells which contain secretory granules within their cytoplasm used to combat infection). While normally circulating free in the bloodstream, the release of chemokines induces chemotactic migration of neutrophils to the target

site and provokes adhesion molecules such as *selectins* to be expressed on the surface of the endothelium. This begins the multistep adhesion cascade of *tethering, rolling, activation* and finally *arrest* which stops neutrophils from circulating and allows them to pass out of the bloodstream into the surrounding tissues.

Once firmly tethered to the epithelium of a capillary, the neutrophil begins the process of *diapedesis*, producing proteases which break down the basement membrane and extending cell-membrane projections (*pseudopodia*) through gaps between the endothelial cells. Interactions between proteins on the surface of the neutrophil and the endothelial cell then pull the neutrophil through the gap into the interstitial fluid.

In an acute inflammatory scenario, fluid, plasma proteins and white blood cells (predominantly neutrophils) enter the tissue causing swelling. The neutrophils then engage the target microbes via two principal mechanisms: *degranulation* and *phagocytosis*. Degranulation involves the secretion of antimicrobial proteins such as lactoferrin and myeloperoxidase (the green-pigmented enzyme which causes the green tint in pus), whereas phagocytosis involves the direct uptake of microbes or particles after which they are killed with bursts of highly oxidising chemicals.

2.3 Apoptotic cell removal

After the threat of invasion has been removed, it is of vital importance that the tissues return to their normal state and function. This involves a reversal of all the processes which instigated the inflammatory response. Haslett [15] lists:

> "removal of the stimuli [which trigger] inflammation; dissipation or destruction of pro-inflammatory mediators; cessation of granulocyte emigration from blood vessels; restoration of normal vascular permeability and removal of extravasated fluids; limitation of granulocyte secretion of pro-inflammatory and histotoxic agents; cessation of monocyte emigration and their maturation into macrophages; removal of fibrin and protein clots, bacterial and cellular debris, and granulocytes and macrophages; and, finally, repair of any 'bystander' injury to constitutive endothelial and epithelial monolayers."

Among this sizeable collection of requirements, the removal of neutrophils is highly significant. The degranulation used to combat infection invariably causes a certain amount of 'collateral damage', but these short-lived cells also have the potential to cause much more damage if their cell membranes break down and release their contents: a combination of cytotoxic chemicals and autoimmunogenic species.

To prevent this, neutrophils first undergo programmed cell death, or *apoptosis*: the cells lose the ability to *degranulate* (release antimicrobial cytotoxic agents in response to inflammatory signals); the cell shrinks and becomes rounded due to the degradation of the cytoskeleton; the nucleus breaks into smaller packets of fragmented DNA and the cell often breaks into smaller *apoptotic bodies*. The cell membrane of the apoptotic cell or apoptotic bodies remains intact, but after only a few hours they will undergo *secondary necrosis* [15]. During necrosis the cell membranes break down releasing their pro-inflammatory and auto-immunogenic contents: proteases, heat-shock proteins, double-stranded DNA and myeloperoxidase. Henson *et al.* also conjecture that mitochondria released from lysed or necrotic cells also contribute to the inflammatory response due to their evolutionary origin as endosymbiotic bacteria [16].

The rate at which neutrophils undergo apoptosis can be influenced by external factors. Apoptosis can be accelerated by UV-irradiation, cycloheximide, tumour necrosis factor α (TNF-α), nitric oxide donors and ligation of the Fas receptor [15, 17]. Neutrophil apoptosis is in turn inhibited by raised levels of extracellular calcium, lipopolysaccharide (LPS), granulocyte macrophage colony stimulating factor (GM-CSF), hypoxic conditions, agents which elevate intracellular cAMP and corticosteroids.

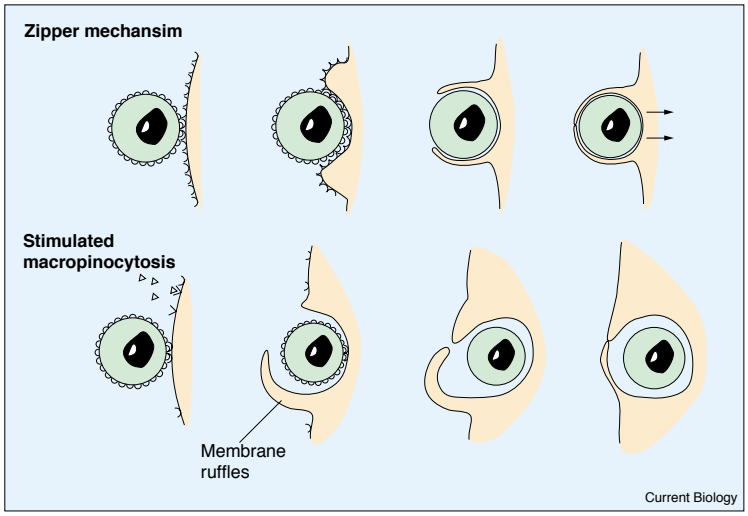

Figure 2: Contrasting mechanisms of ingestion (reproduced from Henson *et al.* (2001) [19])

In order to maintain healthy tissue, then, the body must remove neutrophils from the site of inflammation in the short window period between apoptosis and necrosis. This task is performed by a large number of cell types but chiefly by macrophages and dendritic cells. The differential role of these two cells types is discussed by Xu *et al.* (2006) [18], who list results which imply that dendritic cell uptake of apoptotic cells—especially late apoptotic cells—is more likely to lead to pro-inflammatory antigen presentation. In a healthy, functioning individual the process is extremely efficient: over 10^{11} circulating neutrophils are removed and replaced in a single day, replacing the entire circulating population over two and a half times in that period, and apoptotic cells are found at barely detectable levels.

The specific mechanism of apoptotic cell uptake by macrophages has been termed *efferocytosis*—a name derived from the latin *effero* meaning 'to bury the dead'. In [19] and also an online lecture[3], Peter Henson outlines the morphological differences in categories of cell uptake mechanisms. Small particles (around 100nm) are ingested via pinocytosis without major alterations of the cytoskeleton. Larger particles ($> 1\mu$m) are typically ingested via two contrasting mechanisms: *phagocytosis* or *macropinocytosis*. Phagocytosis is definitively particle-driven, whereby ligands such as antibodies on a particle engages receptors on the macrophage, leading to extension of the cell membrane to envelop the particle and internalise it in a closely-bound phagosome. The early engagement of the surface receptors promotes a partial cell membrane extension which allows binding to further receptors in a chain reaction keeping the cell membrane in close contact with the ingested particle. This characteristic manner of engulfment is often referred to as the 'zipper mechanism'. With macropinocytosis, a long cell-membrane ruffle is extended into the fluid and then reaches round from one side to engulf materials attached to the cell and those in the surrounding fluid, drawing them into a much looser, fluid-filled cavity within the cell.

Henson states that efferocytosis is morphologically more similar to macropinocytosis: the apoptotic cell or apoptotic body first attaches to the macrophage cell surface and then a cell membrane extension engulfs the cell along with surrounding fluid, drawing it into a spacious efferosome. He cites a study where apoptotic Jurkat cells (an immortalised strain of T lymphocytes, frequently used in cellular experiments) deliberately opsonised with immunoglobulin G are ingested via the zipper mechanism into a tight phagosome containing no fluid rather than the larger fluid-filled efferosome observed with normal apoptotic cells.

The success of this resolution phase and the extent of damaging side-effects due to inflammation

[3]Henry Stewart Talks: `http://www.hstalks.com`

is highly variable: Haslett [15] notes that streptococcal infections tend to induce inflammation which resolves completely with few side-effects whereas staphylococcal infections instead provoke persistent inflammation with associated scarring of tissue.

Although research has, until recently, concentrated on the mechanisms by which inflammation is triggered and amplified in order to defend host tissues, considerable interest is now being turned towards the resolution phase since defects in its function are believed to have wide-ranging consequences, particularly in the pathogenesis of a number of chronic inflammatory disorders.

2.4 Chronic disorders

Cell populations within the lungs can be studied by *pulmonary lavage* whereby a tube is inserted into the lung via the nose and a small amount of fluid is first injected and then re-collected for examination. In this type of study apoptotic cells are rarely detected in levels above 1–2% [20]; this is true both for assays of the naïve lung and cases of acute inflammatory conditions such as community-acquired pneumonia or acute respiratory distress syndrome (ARDS).

In chronic inflammatory lung conditions, however, apoptotic cells are frequently found in higher numbers [20, 21]. These include cystic fibrosis (CF), non-CF bronchiectasis, chronic obstructive pulmonary disease, asthma and idiopathic pulmonary fibrosis and a number of the symptoms of these arise from damage caused as a direct result of the inflammation itself. Haslett asserts that one could "be forgiven for considering inflammation as a detrimental process" which consistently causes tissue injury. He and other authors note the paradox inherent in the evolution of inflammation as a host defence mechanism when the mechanism itself has potential do cause significant harm[15, 9].

Possible reasons for increased detection of apoptotic cells in disorders of this type could be: an increased rate of apoptosis, impaired efferocytosis, apoptosis in disproportionally large numbers so normal removal systems cannot cope, or an artefact of the data. Vandivier *et al.* hypothesise that it is impaired efferocytosis which leads to increased numbers of apoptotic cells.

In the case of CF, studies by Vandivier *et al.* show that efferocytosis is suppressed by elastase activity, which inhibits ingestion of the apoptotic cell. They suggest that the elastase enzyme cleaves an as-yet unidentified receptor on the macrophage surface responsible for initiating uptake of the apoptotic cell. Other factors which may also contribute to defective clearance are the retarding effect of thick mucus in the lungs, preventing macrophage chemotaxis towards their targets; low levels of pulmonary surfactants and high levels of pro-inflammatory cytokines such as TNF-α [20].

In COPD patients and animal models, Vandivier *et al.* note that increased numbers of apoptotic cells are found not only in the lungs but also in skeletal muscle tissue, indicating that the defects in cell clearance may be systemic rather than local. They cite studies in which the number of ingested apoptotic cells within alveolar macrophages were counted and found to be below average, strengthening the hypothesis that it is reduced clearance which accounts for the increased number of apoptotic cells. They also note that impaired efferocytosis can be induced in murine models with genetic alterations to inhibit production of pulmonary surfactants or overproduce TNF-α.

Cigarette smoke was also found to suppress apoptotic cell clearance *in vitro* and *in vivo*. This is significant as, in patients with COPD, inflammation can last for a long time after smoking cessation indicating that the inflammation is not merely a direct reaction to the contents of the smoke but the result of damage to normal suppressive mechanisms [21].

Vanidiver *et al.* also note that increased numbers of apoptotic cells are found in chronic inflammatory conditions elsewhere in the body. They cite papers demonstrating impaired clearance in patients suffering from rheumatoid arthritis, systemic lupus erythematosus, glomerulonephritis and atherosclerosis.

3 Signalling mechanisms

3.1 Recognition of target cells

For macrophages to be able to detect and remove apoptotic cells in a large population of different cell types, a large number of receptors and bridging molecules are involved in generating the 'eat-me' signal across what Vandivier *et al.* refer to as the *phagocytic synapse*. The roles of these receptors are diverse: some tether the target cell to the phagocyte and some generate a signal causing membrane alterations which initiate engulfment. Given the fine balance which must be attained it certainly seems sensible for a degree of redundancy in identifying which cells to target: with too few checks in place, the macrophages could potentially target healthy tissues instead of apoptotic cells.

A key pathway is the *collectin* pathway: collectins are a class of pattern recognition molecule which include mannose-binding lectin (MBL) and the surfactant proteins (SP)-A and D. These molecules share a collagen domain which binds to *calreticulin*, a protein usually found in the endoplasmic reticulum to mediate protein folding. On the cell surface, calreticulin acts in partnership with the transmembrane CD91[4] domain to generate a signal initiating uptake of the target cell [22]. The complement protein C1q is closely related to collectins and is also recognised by calreticulin.

Vandivier *et al.* [23] measured the relative importance of SP-A, SP-D and C1q in clearance of apoptotic cells in the murine lung, finding that all species enhanced apoptotic cell ingestion by macrophages *in vitro.* but only the SP-D knockout resulted in a statistically significant loss in clearance *in vivo.*

This result was supported by Clark *et al.* [24] and Palaniyar *et al.* conducted a further study showing that collectin proteins enhance efficient phagocytosis of apoptotic cells and further showed that a second function of collectin proteins, especially SP-D, was to minimise the generation of anti-DNA autoantibodies in response to DNA displayed on the surface of apoptotic cells [25].

Alcorn & Wright (2004) [26] demonstrated that, as well as promoting apoptotic cell uptake, SP-A decreased LPS-stimulated expression of TNF-α in mice and rats, via a lipopolysaccharide-independent pathwas. This shows that high collectin levels have both pro-phagocytic and anti-inflammatory effects.

Gardai *et al.* (2003) [27] note that SP-A and SP-D perform a dual role in modulating lung inflammation: while normally suppressing inflammation by stimulation of signal-regulatory protein α (SIRPα), these surfactant proteins are also implicated in clearance of foreign material in which case they promote phagocytosis which triggers a pro- rather than anti-inflammatory pathway.

A second molecular species which may be involved is the phospholipid *phosphatidylserine* (PS). Normally resident on the inner leaflet of cell membranes, PS is externalised in dense patches during cell apoptosis [16, 19]. The receptor which recognises these PS patches is still unknown but it has been shown that blocking PS expression on apoptotic cells prevents most apoptotic cell uptake *in vitro*. Ligation of the receptor is both pro-phagocytic and anti-inflammatory stimulating efferocytosis and an increase in the anti-inflammatory mediator transforming growth factor β (TGF-β). Henson *et al.* suggest PS-receptor ligation as a 'crucial molecular switch' between pro-inflammatory and pro-resolution macrophage behaviour where binding of PS overrides the default pro-inflammatory role and is in turn overcome by subsequent changes in the environment. Two cases in point are blocking of the PS by proteins such as annexin V or cleavage of the receptor by proteases released from lysed cells.

Mevorach *et al.* (1998) [28] suggest that activation of both the classical and alternative complement pathways via phosphatidylserine exposure was important in apoptotic cell uptake. Activation of the complement pathways leads to deposition of the complement species C3bi on the apoptotic

[4] CD91 is also referred to as low density lipoprotein receptor-related protein 1 (LRP1)

Cytokine	Function	Pro/anti-inflammatory?
IL-1β	Stimulates proliferation of thymocytes and B-cell maturation and proliferation	Pro
IL-8	Attracts and activates neutrophils, basophils and T-cells	Pro
GM-CSF	Stimulates the growth and differentiation of hematopoietic precursor cells including granulocytes, macrophages, eosinophils and erythrocytes	Pro
TNF-α	A potent pyrogen causing fever by direct action or by stimulation of interleukin-1 secretion	Pro
IL-10	Inhibits the synthesis of a number of cytokines, including IFN-γ, IL-2, IL-3, TNF and GM-CSF produced by activated macrophages and by helper T-cells	Anti
TGF-β	Controls proliferation, differentiation, and other functions in many cell types. Downregulates the production of various pro-inflammatory mediators.	Anti

Table 1: Summary of cytokine functions. Sources: UniProt and OMIM

cell surface, which then facilitates uptake via the receptors CR3 and CR4 on the macrophage surface.

Other macrophage receptors implicated in apoptotic cell recognition and uptake include: CD31, MER, αvβ3/5 integrin, CD36, β2-GP1 receptor, CD44 and CD14 [29, 30, 31, 20]

3.2 Regulation of inflammatory response

The effect of recognition and uptake of apoptotic cells is not limited to the active phagocyte: autocrine and paracrine mechanisms alter the behaviour of surrounding macrophages, neutrophils and epithelial tissues.

Fadok *et al.* [32] demonstrate that efferocytosis is not a 'quiet process': production of pro-inflammatory mediators is actively inhibited in human macrophages which have ingested apoptotic cells, whereas production of anti-inflammatory molecules is significantly upregulated. In their study, the authors compared the concentrations of six cytokines (see Table 1), as determined by ELISA[5], in cultures of human macrophages incubated for 18 hours with either apoptotic human neutrophils, immunoglobulin-G-opsonised neutrophils or no stimulus. Six cytokines were monitored: interleukin (IL)-1β, IL-8, granulocyte macrophage colony-stimulating factor (GM-CSF), tumour necrosis factor α (TNF-α), IL-10 and transforming growth factor β (TGF-β). Of these, the concentrations of IL-10, GM-CSF and TNF-α were significantly lower in the apoptotic cell culture than the IgG-opsonised culture and the concentration of TGF-β was significantly higher in the apoptotic cell culture than the opsonsised culture (see Fig 3).

This shows that detection of apoptotic cells by macrophages stimulates an immunosuppressive signal, preventing further influx and activation of neutrophils. Cox describes the effect of IL-10 on clearance of apoptotic cells: in an *ex vivo* study of neutrophils obtained from rats by bronchoalveolar lavage, the addition of IL-10 together with a dose of lipopolysaccharide to stimulate neutrophil

[5]Enzyme-Linked ImmunoSorbent Assay

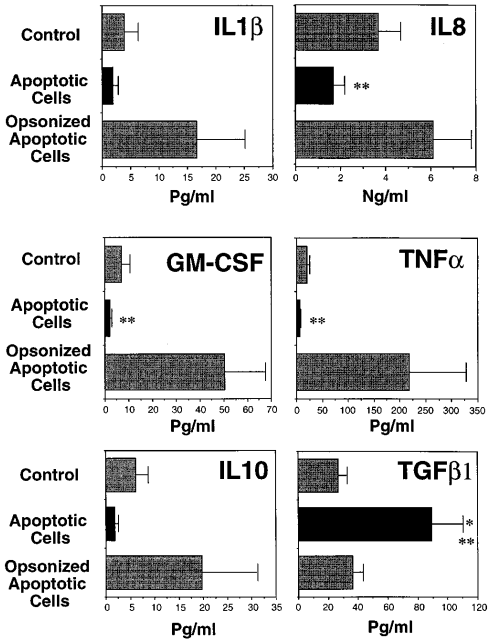

Figure 3: Graph of results reproduced from Fadok *et al.* [32]

response did not affect the onset or peak of neutrophil recruitment but led to swifter macrophage clearance by promoting neutrophil apoptosis and reducing levels of TNF-α [33].

Haslett notes that *in vitro* experiments have shown an improvement in macrophage efferocytosis by agents which modulate macrophage cAMP and by corticosteroids.

Serhan & Savill [11] also suggest a role for arachidonic acid-derived *eicosanoids* in the switch from the inflammation to resolution phase. *Prostaglandins* initially facilitate neutrophil migration to the target site which then alter cells to produce the pro-resolution *resolvins* and *protectins* which prevent the entry of new neutrophils to the tissues and stimulate macrophage clearance mechanisms. This system paints neutrophils in a more responsible light: making arrangements for their own removal rather than spiralling in number until checked by the intervention of regulatory macrophages.

Lambrecht [14] further elucidates the central role of macrophages in maintaining lung homeostasis. As well as controlling granulocyte population numbers, he presents results by Takabayashi *et al.* (2006) [34] defining the role of macrophages in preventing inflammatory flare-ups in the case of small-scale infection. The authors outline a 'homeostatic circuit' in which macrophages kept in an inactivated state, closely tethered to the alveolar epithelium (via αvβ6 expressed on alveolar epithelial cells) are normally able to respond to small numbers of inhaled microorganisms. This suppressed state, however, can be bypassed by engagement of macrophage Toll-like receptors which triggers detachment from the alveolar epithelial cells, loss of the αvβ6-mediated suppresion and expression of pro-inflammatory cytokines. After a few days, interaction with recruited T cells stimulates the activation of latent TGF-β, restoring cell-cell contact with the alveolar epithelium and the previous immunosuppressive state.

Henson *et al.* [19] note that even the regulatory mechanism of TGF-β expression has potential to cause damage. TGF-β promotes fibrosis in tissues [35]: in the healing of skin wounds this forms a useful structural 'scaffold' on which normal epithelial tissue can regenerate. In delicate tissues such as the lung or liver, however, fibrosis can lead to long term loss of function and scarring. They also note that expression of TGF-β has been shown to enhance survival of some parasite species

including *Trpanosoma cruzi*—the cause of Chagas disease.

3.3 Potential therapeutic targets

A better understanding of the various mechanisms involved in both the 'beneficial' apoptosis-driven and 'detrimental' necrosis-driven pathways should provide a number of options for intervention in order to tip the balance in favour of swift resolution with minimal damage to the surrounding tissue.

Haslett [15] and Serhan [11] suggest attempting to counter the effects of neutrophil-survival mediators such GM-CSF and by selectively inducing apoptosis in granulocytes. He cites a study of treatment of asthma with corticosteroids, noting that improvements in the patients' condition were associated with increased numbers of apoptotic bodies found in alveolar macrophages. This may suggest that the clinical improvement may be due, in part, to influence on the rate of apoptosis of eosinophils.

He also warns that disproportionate increase in the rate of apoptosis would overwhelm macrophages and lead to a subsequent wave of secondary necrosis triggering further inflammation. Any stimulation of apoptosis, then, would have to be carefully controlled and possibly coupled with agents to increase the rate of macrophage uptake (ligation of macrophage CD44 receptor has been shown to significantly increase clearance rates). Another option could be to genetically modify other cells in the environment, endowing them with professional capability for efferocytosis so that macrophages are not exhausted by huge numbers of apoptotic cells.

In respect of the possible significance of eicosanoid signalling in the resolution phase of inflammation, Serhan & Savill [11] suggest that dietary supplementation with the much-hyped omega-3 fatty acids could be of benefit. These fatty acids are precursors to a number of lipid mediators which inhibit inflammation and so increased levels in the diet could be a preventative measure to aid timely resolution. They also note that aspirin inhibits the synthesis of pro-inflammatory prostaglandins and triggers the generation of pro-resolution *epimeric* forms of arachidonic acid and omega-3 derived mediators.

Luster *et al.* [36] suggest modulating the migration of leukocytes into tissues as a therapeutic paradigm. Defects in leukocyte adhesion exist naturally which result in recurrent bacterial and fungal infections but harnessing the mechanisms involved in these disorders could provide solutions in inflammatory disorders. They cite the use of an integrin antibody, *natalizumab*, to interfere with leukocyte trafficking in treating Crohn's disease and multiple sclerosis. Clearly, though, a careful balance would have to be struck in inhibiting entry of leukocytes into tissues to prevent complete immune suppression.

Han & Ulevitch (2005) [30] discuss a range of regulatory targets which could be used to limit the scale of inflammatory responses. They concentrate on interfering with signalling via the Toll-like receptors as a means to dampen inflammation. This could be by inducing underexpression of macrophage TLRs or by blocking their function with species that bind to the cytoplasmic domain such as TRIAD3A. They note that expression of anti-inflammatory cytokines, including TGF-β downregulates TLR expression, highlighting another pathway by which TGF-β prevents extended inflammation.

In his overview on dampening of inflammation [9], Henson notes that a key aspect of treating chronic inflammatory diseases could be harnessing the pro-resolution capabilities of TGF-β without triggering its potentially damaging fibrogenic consequences.

4 Model development

4.1 Conceptual planning

A conceptual model of the resolution phase was built up incrementally through reading of the available literature and teleconferencing with Dr. Carol Ogden[6]. Layers of complexity were either added if preliminary runs of the model appeared too simple to produce interesting results or removed if there was insufficient data available to support their inclusion or if increased complexity made the results ambiguous.

The first stage of conceptual development was to define the crudest features of the model: the agents involved and their behaviours and capabilities. From the start, the idea was to model two cell types: alveolar macrophages (AMs) and neutrophils. The neutrophil would apoptose according to a pre-defined lifetime and then become available to the macrophage for efferocytosis. After a further period of time, and if not already cleared, the neutrophil would undergo secondary necrosis which should then trigger pro-inflammatory signalling leading to further influx of neutrophils.

I used Mathematica throughout development of the model to sketch ideas quantitatively from the conceptual plan before implementing them in an agent-based context. In order to build a clear framework of how to schedule events over a number of timesteps, I created an initial 'sketch model' of population dynamics. This featured a fixed population of macrophages and a population of neutrophils which aged each timestep, becoming apoptotic and then necrotic and triggering the introduction of new neutrophils as a function of the number undergoing necrosis at each timestep (code and some results are in Appendix C.1).

The nature of the environment in which the agents should move was not clear at the outset. When first experimenting with the development toolkit, I used a two-dimensional toroidal environment as a first approximation and, since the cells are moving on the inner surface of a roughly spherical alveolus, this is in fact a more accurate portrayal of their movement in the real system than, say, 'swimming' in a three-dimensional space. The toroidal environment was the space that was chosen to be used for the final model.

The conceptual model was implemented in the Java programming language, using a library of classes designed for agent-based modelling called MASON[7]. This provides a large number of pre-defined classes for scheduling events, defining steppable objects, comparing objects by location and generating random numbers as well as displaying portrayals of the agents in the model and providing controls for running simulations and charting output. Early stages of this model development allowed me to become more familiar with Java and the MASON toolkit and to develop a base structure from which more complicated behaviours could be constructed.

MASON can be run in either a GUI or non-GUI mode. The classes which provide for these functions are `GUIState` and `SimState` respectively. `SimState` defines the nature of the environment that the agents move in (continuous or discrete, two- or three-dimensional etc.); provides methods to start, stop and load simulations; and instantiates and schedules the agents which are to be involved in the model. `GUIState` overrides the start, stop and load functions of `SimState`, allowing them to be controlled by a graphical console and also handles the portrayal of agents as graphical objects in a display window. Running the `GUIState` object is very useful in development and demonstration, where agent behaviour can clearly be seen and understood in its biological context. The `SimState` mode runs significantly faster, however, making it a more powerful tool for generating sufficient data for statistical analysis, provided suitable output methods are written into the class.

[6] Epithelial Cell Response and Repair Research Group, GlaxoSmithKline, Philadelphia

[7] Multiagent simulation toolkit: `http://cs.gmu.edu/~eclab/projects/mason/`

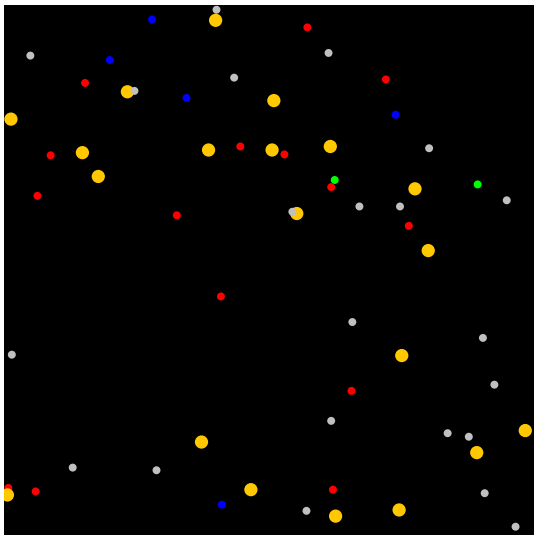

Figure 4: Screenshot of MASON display

4.2 Agent movement and changes of state

My first package, `toroidal`, sought simply to model the simplest aspects of the conceptual model: agent movement, apoptosis, necrosis and efferocytosis and for these events to be portrayed in the GUI in a clear manner.

A chosen number of macrophage and neutrophil agents (defined by the `Macro` and `Neutro` classes in the package) are initialised at random locations and with random initial directions in the environment. The macrophages are distinct from the neutrophils with their larger diameter and are coloured orange. The neutrophils are coloured grey. Changes in the neutrophil's colour indicate its state. Upon apoptosis, the neutrophil turns red and upon necrosis it turns green. The time taken for the neutrophil to apoptose is a uniformly distributed random number whereas necrosis occurs a fixed number of timesteps after apoptosis.

Since efferocytosis is dependent on the mediation of a chain of molecular interactions (the collectin or perhaps phosphatidylserine pathways), apoptotic agents are not available for removal by the macrophage agents until 'bound' by an opsonising molecule. This binding event may occur each timestep with a fixed probability. Neutrophils bound with collectin are coloured blue in the GUI display and are available for efferocytosis by the macrophage agents. Figure 4 shows the GUI display with neutrophil agents in the various states.

Although in reality a large number of receptors and bridging molecules are involved in the recognition of apoptotic cells, the model simplifies the recognition process so that macrophage agents ingest any apoptotic neutrophil agent which has been bound with collectin.

In this package, all agents move in straight lines, wrapping around the environment when they reach a boundary. There is a `collision()` method in the simulator which is called if two agents come close enough to touch. Usually the agents bounce off each other but a macrophage will ingest either collectin-bound apoptotic or necrotic cells, removing them from the simulation.

The algorithm followed by the macrophage agents in this package is very simple: each timestep, the agent calculates its new position; changes its 'internal' coordinates to this position; updates its location in the simulation environment to the same position and then determines whether it has collided with another agent. This is shown schematically in Figure 5.

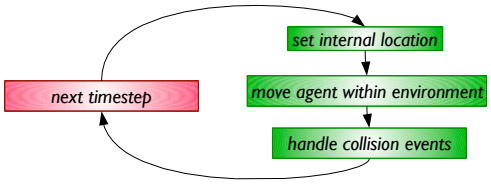

Figure 5: Diagram of methods in `Macro` agent which are run each timestep in the `toroidal` package

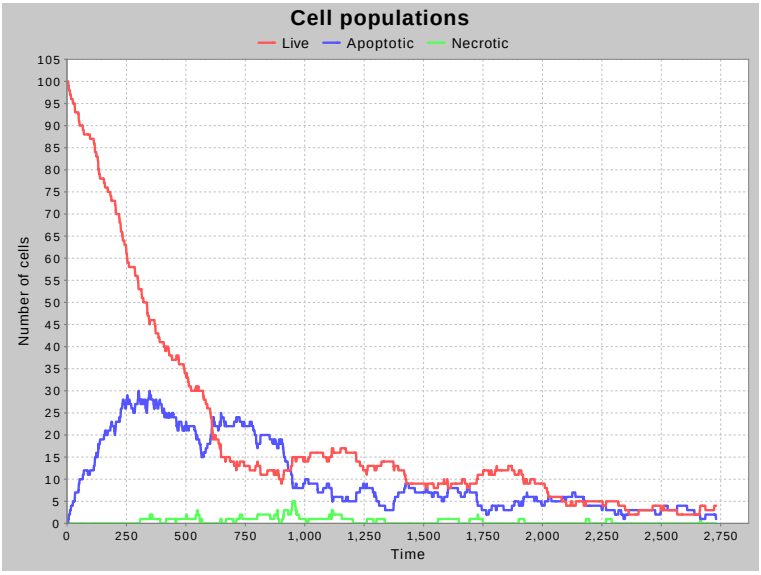

Figure 6: MASON's charting capabilities

4.3 Macrophage chemotaxis

In consultation with Carol Ogden, it was agreed that the macrophages should have a chemotactic component to their movement. In the `chasers` package, I implemented an extra method in the `Engine` class which is called by the `Macro` agents in which they change their angle of movement each timestep based on a combination of their current direction, attraction towards nearby opsonised or necrotic agents and repulsion by other macrophages. The mathematical details are shown in Appendix A.1.

With this addition to the code, the macrophage agents smoothly change direction towards nearby ingestible cells and avoid bumping into one another, resulting in a more lifelike appearance than the 'billiard ball' dynamics of the `toroidal` package.

As well as a graphical portrayal of the entire simulation, MASON also provides simple methods to access variables in the code and stream or chart them via the GUI. In this package I added several variables to keep track of the number of neutrophils which were live, apoptotic (either bound or unbound by collectin) and necrotic. Figure 6 shows an example chart of cell populations from a single run of the model.

Adding a change of direction based on chemotactic signals required adding an extra method called by the macrophage each timestep. Figure 7 shows the sequence of methods called each timestep in the `chasers` package.

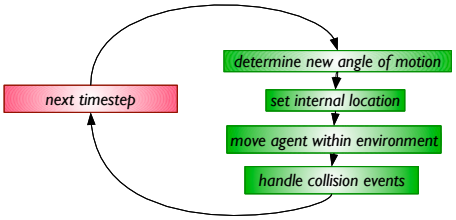

Figure 7: Diagram of methods in `Macro` agent which are run each timestep in the `chasers` package

4.4 The signalling model

The `hybrid` package builds in cell signalling as a modulator of agent behaviour. Exposure, whether it is via close proximity or actual ingestion, of macrophages to apoptotic cells should elicit a pro-resolution response via expression of cytokines such as IL-10 and TGF-β. In the paper by Fadok *et al.* [32], pro-inflammatory signalling was stimulated by presentation of apoptotic cells opsonised with IgG, which promotes phagocytic rather than efferocytic uptake. The authors cite an earlier study in which macrophage engulfment of necrotic eosinophils was shown to stimulate pro-inflammatory signalling (particularly upregulation of GM-CSF) but note that attempts to reproduce these results with necrotic neutrophils were inconsistent, sometimes stimulating a pro-inflammatory response and sometimes eliciting no response. For the purpose of the model, it is assumed that exposure to necrotic neutrophils does indeed trigger inflammatory signalling, and the data from the IgG-opsonised apoptotic cells is used as a stand-in for the lack of data on necrotic cells.

Various combinations of cytokine types were considered but, due to lack of detailed studies on how each regulates expression of the other, it was decided to only monitor the production and effect of two signalling molecules: one pro-inflammatory and one pro-resolution. The pro-inflammatory signal can be considered to be either TNF-α or GM-CSF and the the pro-resolution signal either TGF-β or IL-10. They are hereafter referred to as TNF-α and TGF-β and the data from the Fadok paper on changes in TGF-β and TNF-α are used to parameterise the model (see §4.5). The number of new neutrophils initialised each timestep is then a function of the resultant concentrations of the pro- and anti-inflammatory signalling molecules. A diagram of this signalling/behaviour scheme is shown in Figure 8.

Macrophage agent behaviour is a result of the proportion of occupied receptors at any one timestep. The receptor dynamics is based on very simple textbook recurrence relations [37] in which free ligand in the surrounding medium binds to a cell-surface receptor in proportion to the concentration of ligand in the surrounding medium and the number of unoccupied receptors and the number of ligands dissociating from the receptors is proportional to the number of occupied receptors (see Appendix A.2). Ligand-receptor association and dissociation are respectively regulated by rate constants k_+ and k_- and the total number of cell surface receptors is constant, i.e. receptor generation, internalisation and recycling mechanisms are not considered in this model.

The concentration of the two signalling molecules is treated as a constant across the entire medium, but receptor dynamics by which macrophage agents detect apoptotic and necrotic cells is based on local information. This could be modelled by two-dimensional diffusion of some kind of recognition molecule giving a spatially-varied concentration value but I used a somewhat simpler mechanism: the macrophages simply count the number of agents of each type within a fixed distance during the chemotaxis calculation step and the totals are summed over the last 100 timesteps. This provides for a more slowly varying concentration value than simply basing it on the surroundings in the current timestep.

We wish the production of signalling molecules to depend on the relative number of receptors occupied detecting apoptotic or necrotic cells. The detection of apoptotic cells should inhibit the

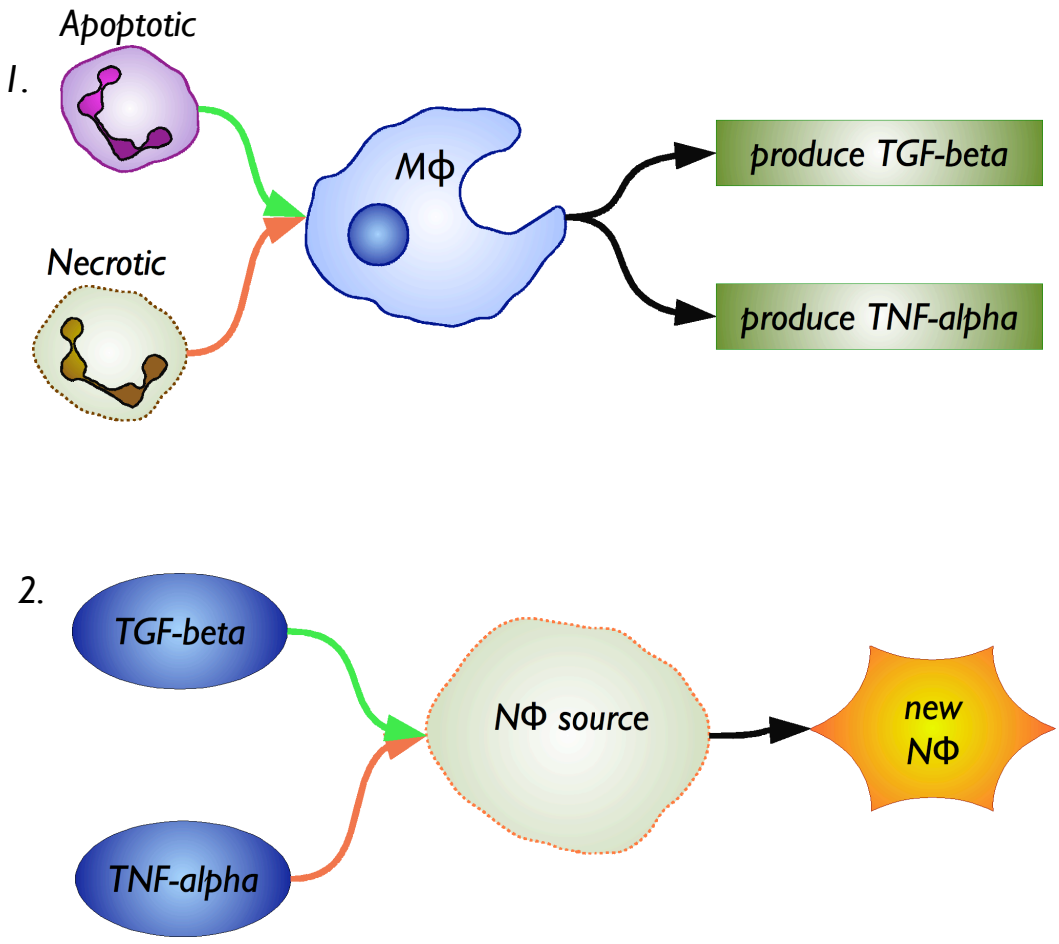

Figure 8: Diagram of interactions in `hybrid` package

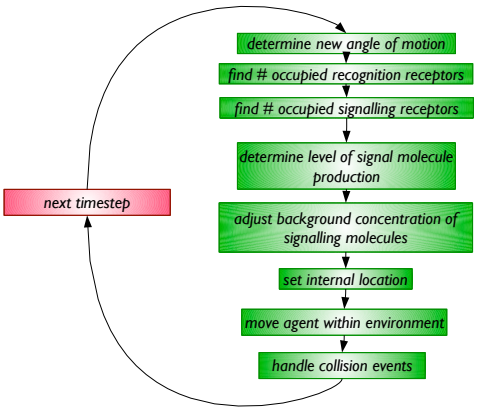

Figure 9: Diagram of methods in `Macro` agent which are run each timestep in the `hybrid` package

production of pro-inflammatory signals and, likewise, detection of necrotic cells should inhibit production of pro-resolution signals. Since the concentrations of signalling molecules are shown to be nonzero in the control groups tested in Fadok *et al.* [32], there should be a 'homeostatic' rate of production of both signalling molecules when there is no stimulus.

To satisfy these conditions, we wish to define productivity functions $P^\beta(R^\beta, R^\alpha), P^\alpha(R^\beta, R^\alpha)$ such that:

$$P^\beta = \begin{cases} P^\beta_{hom} & , \quad (R^\beta, R^\alpha) = (0,0) \\ P^\beta_{max} & , \quad (R^\beta, R^\alpha) = (100,0) \\ 0 & , \quad (R^\beta, R^\alpha) = (0,100) \end{cases} \quad \text{and} \quad P^\alpha = \begin{cases} P^\alpha_{hom} & , \quad (R^\beta, R^\alpha) = (0,0) \\ P^\alpha_{max} & , \quad (R^\beta, R^\alpha) = (0,100) \\ 0 & , \quad (R^\beta, R^\alpha) = (100,0) \end{cases}$$

For the purposes of this model I used a simple linear combination of the proportion of occupied receptors (see Appendix A.3). A more biologically plausible productivity function would be a 'saturating' hyperbolic form such as:

$$P = \frac{P_{max} F}{F_{half} + F}$$

where the productivity tends to P_{max} as the stimulus intensity F increases to infinity and where F_{half} denotes the value of F which elicits a value of $\frac{1}{2} P_{max}$.

A final method then calculates the variation in background concentration depending on the number of receptor-ligand binding and dissociation events, the rate at which signalling molecule is being produced by the agent and a degradation constant k_{deg}, representing the rate at which signalling molecules disperse, decompose or are recycled by cells in the environment (see Appendix A.4).

This mechanism adds a further four methods to be called by the macrophage each timestep as illustrated in Figure 9.

This package also included a new class: `StemCell`. This slightly misleadingly named class is a steppable agent like the macrophage and neutrophil agents but is not portrayed in the simulation. It calls the methods in the base simulation to create a new neutrophil agent based on similar receptor dynamics to those used in the macrophage agents. The association and dissociation constants for the two signalling molecules are the same as the macrophages and the function translating receptor occupation to a probability is similar to the linear combination in Appendix A.3:

$$p\{new\ neutrophil\} = p_{max} k_{hom} \left(1 + \left(\frac{1 - k_{hom}}{k_{hom}}\right) \frac{R^\alpha}{N^\alpha} - \frac{R^\beta}{N^\beta}\right)$$

Brief experimentation led me to choose homeostatic and maximum values for neutrophil influx which provided a wide range of potential outcomes without any extreme behaviour. The values chosen were $p_{max} = 0.05$ and $k_{hom} = 0.001$.

4.5 Choosing parameter values

An important consideration before running the model was how much effort to put into tying parameter values as closely as possible to observed data. Since the model is fairly abstract in comparison to the living system it is not always desirable to simply 'plug in' the various measurements which can be mined from the data. In many cases, sufficiently detailed experimental results are not currently available. The approach I took was to use a number of authoritatively-defined global-level parameters as constraints and elsewhere to use more-or-less arbitrary values which produced qualitatively reasonable behaviour.

The paper that I felt had the most accessible and relevant experimental results was that of Fadok *et al.* (1998) [32], which measured expression of pro- and anti-inflammatory mediators in response to various stimuli. I used the end-point concentrations of TGF-β and TNF-α as characteristic parameters from which to derive values for the various rate constants used in the `hybrid` package.

I assumed that the values reached after the 18 hour experiments were equilibria at which both the number of cell-surface receptor complexes and the concentration of signalling molecules were unchanging. Let C^{β}_{max} and C^{β}_{hom} denote the equilibrium concentrations of TGF-β in the surrounding medium under maximum stimulation (all receptors occupied) and under no stimulation. If the concentration and number of surface-receptor complexes are both unchanging then, in the maximal case, we have:

$$P^{\beta}_{max} + k^{\beta}_{-}\frac{R^{\beta}}{N^{\beta}} - k^{\beta}_{+}C^{\beta}_{max}\left(1 - \frac{R^{\beta}}{N^{\beta}}\right) - k^{\beta}_{deg}C^{\beta}_{max} = 0$$

$$k^{\beta}_{+}C^{\beta}_{max}\left(1 - \frac{R^{\beta}}{N^{\beta}}\right) - k^{\beta}_{-}\frac{R^{\beta}}{N^{\beta}} = 0$$

Which combines to give:

$$P^{\beta}_{max} = k^{\beta}_{deg}C^{\beta}_{max}$$

Since the available data is end-point concentrations rather than timecourse variation in concentration, it is difficult to choose values for constants which determine rates of expression and degradation. Moreover, no specific attempt has been made to define what a single timestep represents. In light of this, there was some freedom of choice for rate constant values and so I chose an arbitrary value of 0.0015 for k^{β}_{deg}. Using C^{β}_{max} as 90 pg/l from the Fadok *et al.* (1998) results constrains the value for P^{β}_{max} to be 0.135.

A similar derivation gives P^{β}_{hom} as 0.045 and hence:

$$k^{\beta}_{hom} = \frac{P^{\beta}_{hom}}{P^{\beta}_{max}} = 0.333$$

I also decided that homeostatic concentrations of both signalling molecules should correspond to 10% receptor occupation. Denote this number by R^{β}_{hom}. This gives us the relation:

$$k^{\beta}_{+} = \frac{k^{\beta}_{-}R^{\beta}_{hom}}{N^{\beta}C^{\beta}_{hom}\left(1 - \frac{R^{\beta}_{hom}}{N^{\beta}}\right)}$$

i.e. k^{β}_{+} and k^{β}_{-} are scalar multiples of one another. By the same reasoning as above, I chose an arbitrary value of 0.5 for k^{β}_{-} giving k^{β}_{+} as 0.00185.

A similar working gives the parameter values for the TNF-α-related entities, which are shown in Appendix A.5.

When it came to defining physical dimensions, it was harder to simply read in figures from the literature. The radius of a single alveolus is around 0.1mm. If we assume it is perfectly spherical this gives an internal surface area of 0.126mm^2. To define a square environment in the model with the same surface area we should use a square with sides of length 0.354mm.

The approximate diameters of macrophages and neutrophils are 20μm and 10μm respectively and a single alveolus at peak inflammation would contain 50–100 resident macrophages[8] and around four times as many neutrophils as well as other extravasated white blood cells. Using these values as a basis for the model, however, results in extremely cramped conditions with unnatural artefacts in the movement of the agents. Of course, cells are not really solid discs moving smoothly on a flat surface like hockey pucks. Their plasticity allows them to pass between other cells when in cramped conditions and they will move over each other as well as on the epithelial wall. Since this model does not provide for such types of movement, it would not be realistic to force the agents into such a small environment.

In the testing stage, I ran the simulation with only 20 macrophages and an average of 100 neutrophils and set the macrophage and neutrophil diameters to 5 and 3 units in a 200 by 200 unit environment. This would correspond to macrophages of diameter around 9μm and neutrophils of diameter 5μm and with population numbers at about half those of the real system.

Commented code for the `batch` package is available for download online at `http://www.ucl.ac.uk/~ucbpeal/sumproj`.

4.6 Model output

Whilst MASON's GUI display is extremely useful in demonstrating individual runs of the model and observing behaviour during the development phase, it is too slow to be used to generate large amounts of data suitable for statistical analysis. For this purpose, output methods need to be written into the base simulator which bypass the graphical console.

The `batch` package added file writing methods to the `hybrid` package and a test which stops the simulation automatically after 5000 timesteps. This was a time period after which variables had typically returned to their equilibrium state when 'normal' parameters were used. Running the base simulator without the GUI on top reduced the time required to simulate 5000 timesteps from several minutes to only one or two seconds.

The MASON framework already provides a command-line argument to run a simulation multiple times and makes the job number accessible by the simulation. The job number was accessed by the simulation both to number the output files distinctly for each run and to increment a particular parameter automatically after a fixed number of runs.

Two output files are written with each simulator run: one to record model-level data and one to record data specific to the macrophage agents. Table 2 shows the variables which are written to file every 50 timesteps during the course of the simulation.

[8] From discussions with Carol Ogden

Model variable	Description	Agent variable	Description
`numNeutros`	Total number of neutrophils	`numApopEaten`	Number of apoptotic cells ingested
`numLive`	Number of live neutrophils	`numNecEaten`	Number of necrotic cells ingested
`numApop`	Number of apoptotic neutrophils (bound or unbound)	`RApop`	Number of occupied 'apoptotic cell receptors'
`numNec`	Number of necrotic neutrophils	`RNec`	Number of occupied 'necrotic cell receptors'
`neutroProb`	Percentage probability a new neutrophil is introduced per timestep	`RBeta`	Number of occupied TGF-β receptors
`CBeta`	Background concentration of TGF-β	`RAlpha`	Number of occupied TNF-α receptors
`CAlpha`	Background concentration of TNF-α	`PBeta`	Production level of TGF-β
		`PAlpha`	Production level of TNF-α

Table 2: Variables written to output files in `batch` package. Left: model-level variables, right: macrophage variables

Parameter	Default value	Min value	Max value	Increment
Number of neutrophils	100	60	150	10
Collectin level	1.0	0.2	2.0	0.2
Max TNF-α	0.333	0.1	1.0	0.1
Max TGF-β	0.135	0.05	0.5	0.05
Velocity	1.0	0.1	1.0	0.1

Table 3: Parameter values used in testing of model

5 Results & analysis

5.1 Model runs

There are a huge range of potential ways to test the model in order to test hypotheses or investigate sensitivity to small changes in parameter values. As an initial investigation of the parameterisation and a demonstration of the type of data which can be extracted I chose five properties which could potentially affect the efficiency of cell-clearance either by modulating the rate at which neutrophils are ingested or otherwise. The five properties which I chose to vary were:

- The starting population of neutrophils: this is to ascertain the impact of the initial scale of the inflammation on the macrophages' ability to return the lungs to normal conditions. A hypothesis for the inability of macrophages efficiently to perform efferocytosis is that they are overwhelmed by large numbers and cannot bring the system back to its homeostatic level before an inflammatory feedback loop is instigated.
- The concentration of collectins in the environment: this is represented by the probability parameter `opsoninLevel`. Underexpression of surfactant proteins were shown to lead to impaired efferocytosis in *in vivo* experiments [23] so assessing the importance of this factor in the context of the computer model is an obvious choice. In this simulation, lower collectin levels will prevent apoptotic neutrophil from being available to macrophages for efferocytosis making them more likely to undergo necrosis before they are cleared.
- The maximum production levels of TNF-α and TGF-β: a possible mechanism for increased numbers of apoptotic cells in chronic disorders is defective macrophage signalling rather than defective phagocytosis. This could be due to overexpression of inflammatory signals or underexpression of signals to inhibit further inflammation. The values changed were the parameters `PAlphaMax` and `PBetaMax` in the `Macro` agent.
- The velocity of cell movement: Vandivier *et al.* suggest that the thick mucus in the lungs of CF patients could prevent macrophages from reaching apoptotic cells quickly enough. Decreasing the speed at which the agents move provides a way to investigate this hypothesis.

Table 3 shows the parameter values used in the runs. Testing of each parameter resulted in 400 ouput files: 200 of model data and 200 of data from each of the 20 `Macro` agents.

5.2 Neutrophil population

For a quantitative understanding of efferocytosis performance we require quantitative measures of various characteristics of the system so that different runs can be compared. Serhan & Savill [11] mention using the time taken for the number of inflammatory cells to fall from its peak value to half that number—essentially the half-life of the resolution process—as a comparative 'index of resolution' in statistical analysis of studies in inflammation.

The first run of the efferocytosis model involved varying the starting number of neutrophils from 60 to 150. Using a Mathematica script, I calculated the average population sizes for the timecourse and used a linear interpolation to estimate the time at which the total number of neutrophils fell

to half its initial value. Figure 10 shows the results of this test.

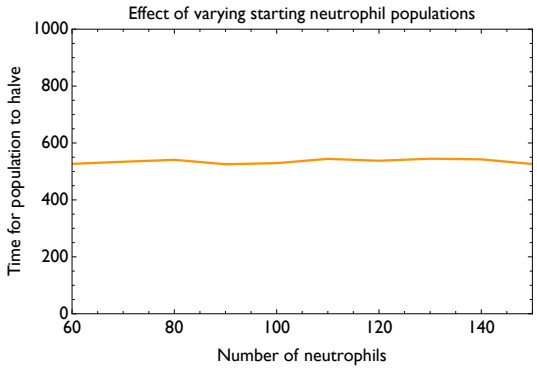

Figure 10: Variation in time required for neutrophil population to halve as initial numbers are incremented

In the range of values tested, there is little to no variation in the time taken for the population of inflammatory cells to halve, the resolution half-life being just over 500 timesteps in each case.

I also plotted timecourses of average values for population size, probability of new neutrophils being introduced and the background concentrations of TGF-β and TNF-α. These are in Appendices B.1–B.4. Of all the parameters varied, changing the initial scale of inflammation appears to have least effect on the long-term state of the simulation: all variables end up at roughly the same homeostatic level. It did, however, appear to have an effect on the peak TNF-α concentration, which peaked at just over 30pg/l with the 60 neutrophil simulations but reached 60pg/l during the 150 neutrophil simulations. The peak occurred at the same point in time in all runs at around 500 timesteps.

5.3 Collectin levels

The effect of lowering the value of `opsoninLevel` was much more pronounced. In this case there was a clear trend of increased time taken for cell numbers to halve as the level of collectins was decreased, with a very sharp increase in the drop from 0.4 to 0.2.

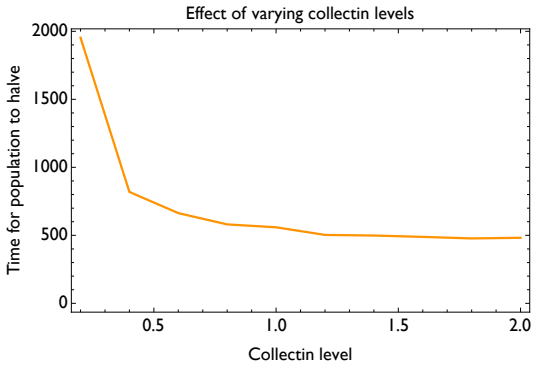

Figure 11: Variation in time required for neutrophil population to halve as `opsoninLevel` is incremented

The concentration of TNF-α and the rate of neutrophil recruitment were also markedly increased in simulations with low collectin levels, both peaking higher and also not returning to the homeostatic levels within the timeframe of the simulation.

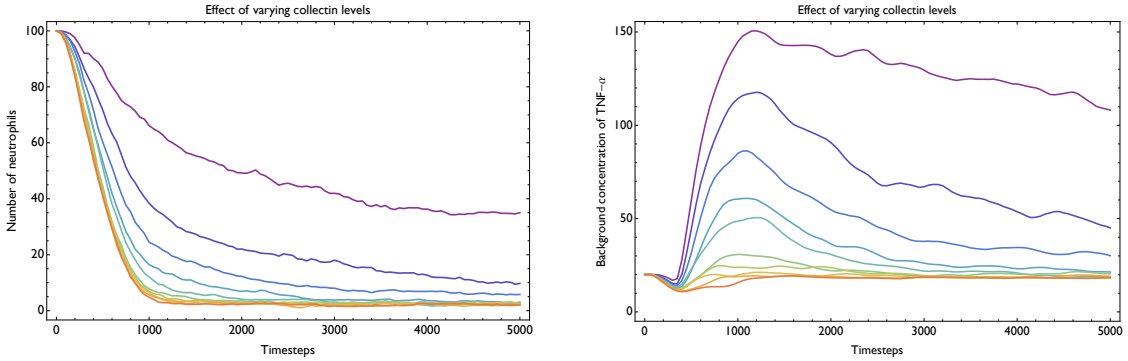

(a) (b)

Figure 12: Reduced rate of resolution in simulations with low collectin levels shown in persistently high neutrophil populations and concentrations of pro-inflammatory mediators (purple: `opsoninLevel = 0.2`, red: `opsoninLevel = 2.0`)

5.4 TGF-β production

The variation of the macrophage levels of TGF-β production also had very little effect on any parameter other than the final steady-state TGF-β concentrations. The time taken for cell populations to halve was unchanged for the parameter values tested (see Figure 13).

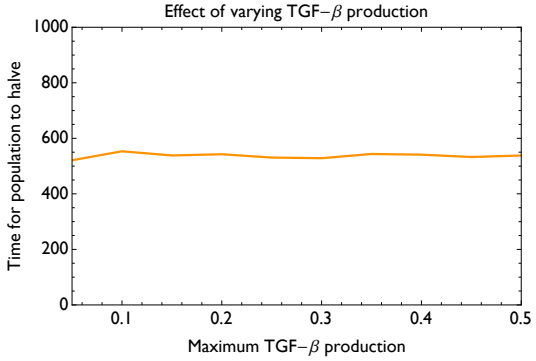

Figure 13: Variation in time required for neutrophil population to halve as `PBetaMax` is incremented

The cell population timecourses were almost identical for each value of `PBetaMax`. The peak values of TNF-α concentration and neutrophil recruitment were lowest when the TGF-β production was at its lowest—this is counterintuitive since TGF-β production should inhibit neutrophil recruitment.

5.5 TNF-α production

When maximum levels of TNF-α production were incremented, there was no change in the time taken for neutrophil numbers to halve, but the steady-state population of neutrophils reached at around 1100 timesteps was larger for higher production of TNF-α (Figure 14).

Increased production levels of TNF-α also, trivially, led to higher concentrations of TNF-α and neutrophil recruitment (see Appendix B for details).

5.6 Speed of chemotaxis

Along with collectin levels, varying the speed of macrophage and neutrophil chemotaxis had greatest effect on the outcome of the simulations. This also showed a generally increasing trend in the

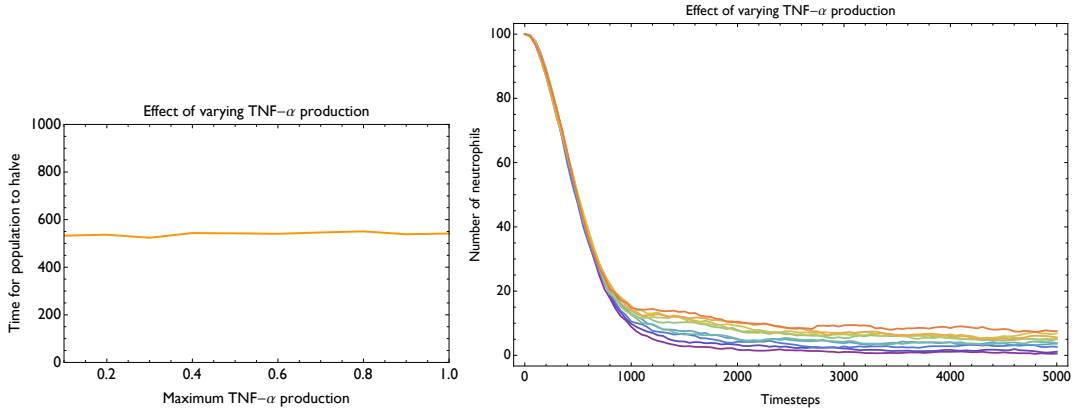

(a) (b)

Figure 14: Variation in time required for neutrophil population to halve as `PAlphaMax` is incremented (purple: `PAlphaMax = 0.1`, red: `PAlphaMax = 1.0`)

required time period as the velocity was decreased, with a sharp change between the two lowest values (Figure 15).

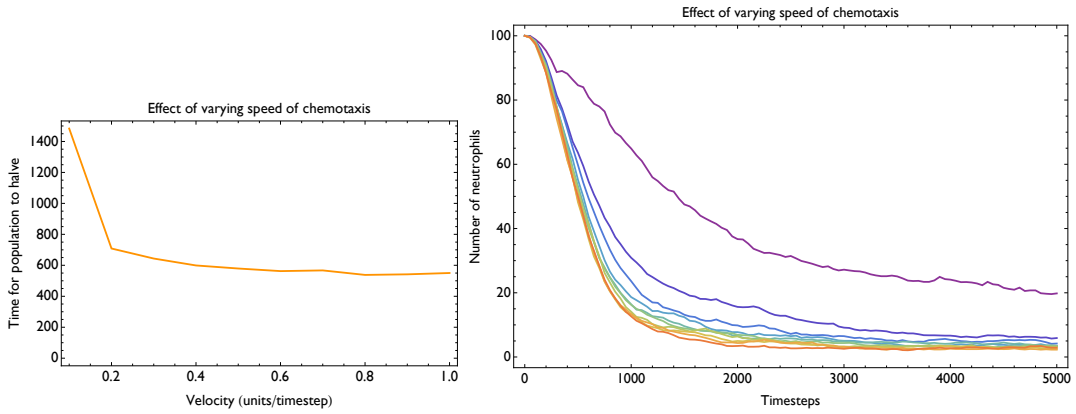

(a) (b)

Figure 15: Variation in time required for neutrophil population to halve as speed of chemotaxis is incremented (purple: `velocity = 0.1`, red: `velocity = 1.0`)

Slowing the speed of the agents also resulted in increased concentrations of TNF-α and increased neutrophil recruitment. TGF-β concentrations were also affected: the peak in concentration was earlier and sharper at lower speeds and led to a higher steady-state concentration: around 50pg/l for a speed of 0.1 and only 36 for a speed of 1.0.

5.7 Point steps in cytokine concentrations

In order to investigate therapeutic interventions I also tried runs of the model where the system was allowed to reach an approximate homeostasis and then the extracellular concentration of TNF-α or TGF-β was instantaneously stepped by a range of different values.

In the TNF-α case, I set all parameters to their 'normal' value (Table 3) and, after 2500 timesteps, stepped the TNF-α concentration by a fixed value ranging from 60–100 pg/l.

This concentration spike is seen directly in the output graph of the TNF-α concentration (Figure 16) and its effects on the neutrophil recruitment signal. Both variables quickly return to the home-

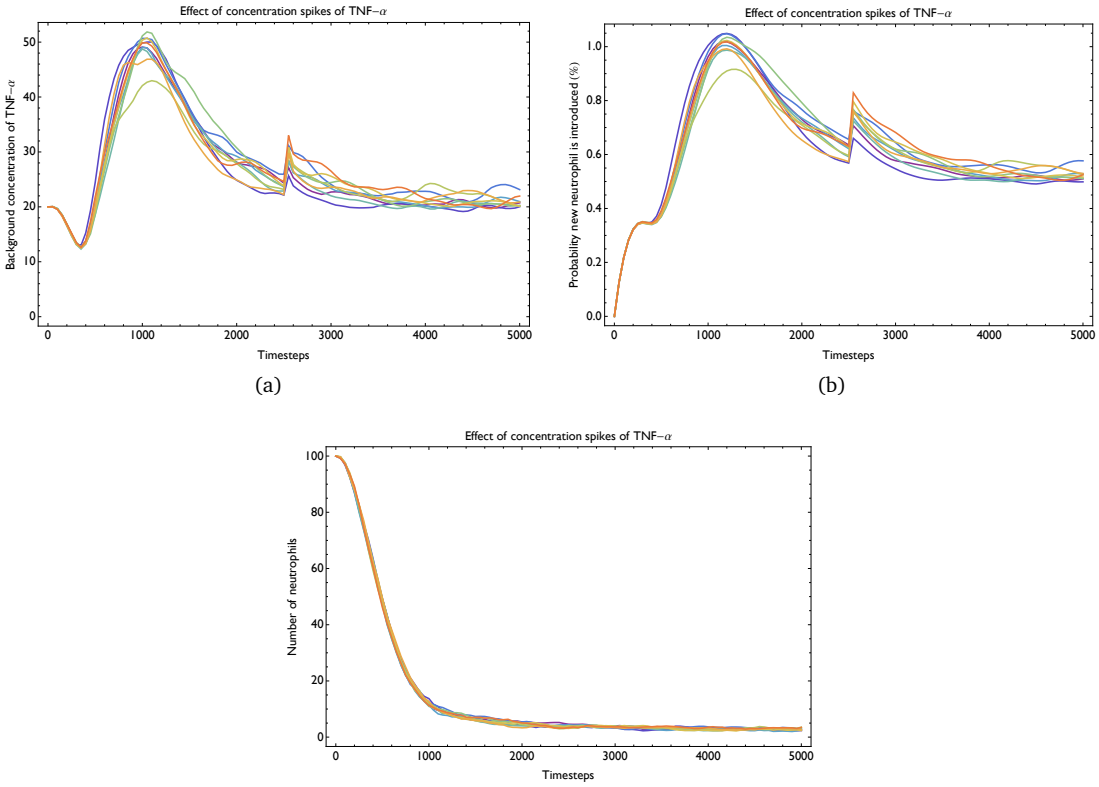

Figure 16: The effect of stepping TNF-α concentrations by values between 60 (purple) and 150 (red) pg/l on the timecourses of TNF-α concentration, neutrophil recruitment and total neutrophil numbers

ostatic level, however, and the increased recruitment signalling is not sustained for long enough to produce a visible increase in neutrophil numbers.

I also stepped the concentration of TGF-β in a system which was displaying symptoms of chronic inflammation (engineered by using the simulation with `opsoninLevel` set to 0.1). Then the concentration was stepped by between 60 and 150 pg/l at the 2500 timestep mark to see whether this would inhibit neutrophil influx enough for the macrophages to 'catch up' with the task of clearance.

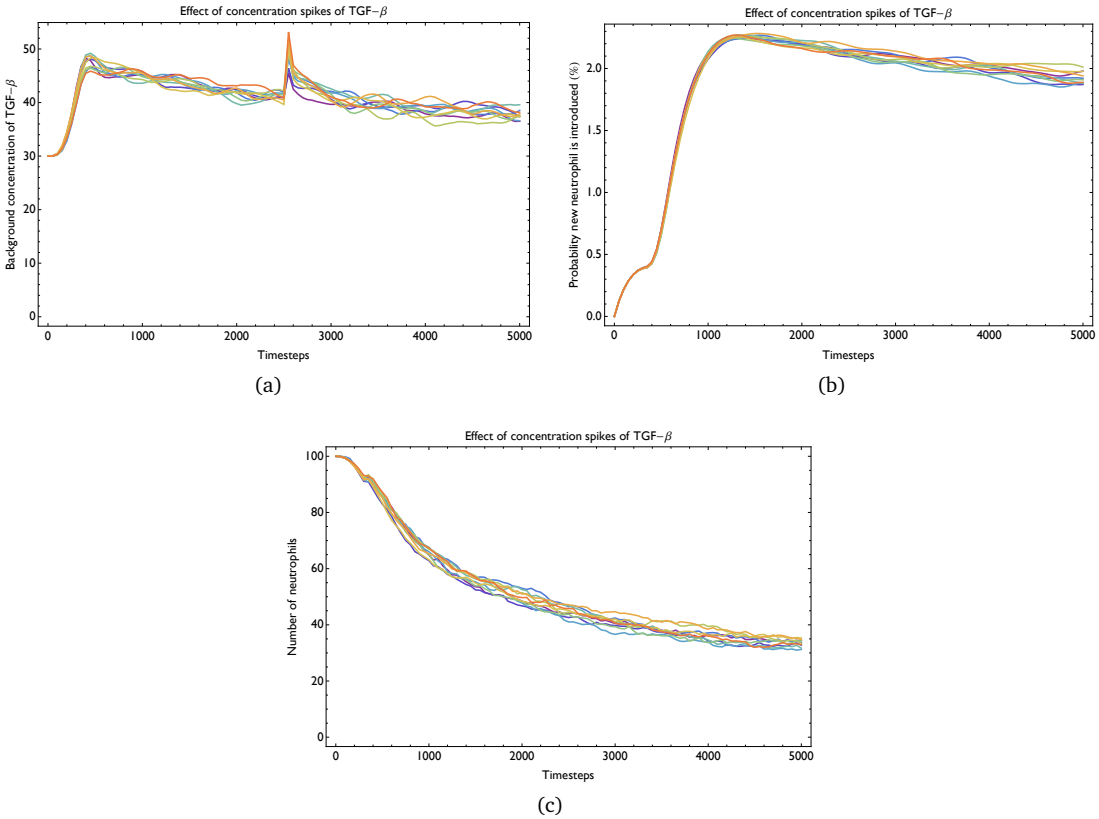

Figure 17: The effect of stepping TGF-β concentrations by values between 60 (purple) and 150 (red) pg/l on the timecourses of TGF-β concentration, neutrophil recruitment and total neutrophil numbers

Again the spike is clearly visible in the concentration timecourse (Figure 17), but the expected inhibition of neutrophil recruitment is not seen in the next graph and there is no modulation of the chronically inflamed state seen Figure 17(c).

6 Discussion

The consensus in the literature cited above is that it is reduced efficacy of clearance mechanisms which contributes to high residual populations of neutrophils and larger numbers of apoptotic cells. This places macrophage performance at the centre of the resolution problem. It should be noted, however, that defective clearance does not necessarily imply an intrinsic macrophage defect, but could also arise as a result of an environmental change which stacks the odds against the macrophage population.

Our results support this perspective: that it is low levels of collectin and impedance of cell movement which have most potential to instigate a chronically inflamed state. In both cases, individual

macrophage behaviour is not defective but the number of efferocytosis events are reduced because of either a break in the chain of recognition or adverse environmental conditions. This leads to increased numbers of necrotic cells and higher neutrophil numbers both because clearance is slower and because the exposure of macrophage agents to necrotic cells provokes higher concentrations of TNF-α, increasing further neutrophil recruitment.

While the variation in pulmonary surfactants as a modulator of efferocytosis performance is a relatively well-studied factor in impaired clearance, there has been little investigation of the possible effects of inhibiting cell movement either on its own or in conjunction with compounding factors. Modelling using ABM encourages consideration of a system in its spatial context, making it a convenient tool for investigating the effect of combining individual agent dynamics with signalling behaviour on global-level outcomes.

Despite the implication of the above simulations that variation in signalling molecule expression and initial scale of inflammation do not significantly affect the speed of resolution, the results must be interpreted with respect to the behavioural features written into the model. A number of potential features were not included in this version which could have the potential to enable variation of these parameters to have a greater influence.

In this simulation, macrophages are able to ingest limitless numbers of both apoptotic and necrotic cells. In reality, there is a limit on the number of cells which can be ingested at one time, after which the macrophage enters a resting period to digest the cells. Although the results above appear to rule out initial population size as an important factor in pathogenesis of chronic inflammation, imposing a limit on the number of cells which could be digested would provide a potential mechanism for large scale inflammation to exhaust the macrophage population and reduce the efficacy of the resolution mechanism, leading to the extended residual populations of neutrophils seen in the other runs.

The macrophages in the simulation were also indiscriminate about whether they ingested apoptotic or necrotic cells. In reality they specialise either in phagocytosis of bacteria and necrotic particles or efferocytosis of apoptotic cells so there are essentially two populations of macrophages which act exclusively as pro-inflammatory or pro-resolution agents[9]. An interesting further investigation would be whether it is more efficient for macrophages to differentiate to an extreme where they ingest only apoptotic or only necrotic cells or to perform multiple functions at a less than professional level.

Modulation of signalling levels also appeared to have little effect on the time for inflammation to resolve. It was surprising that overexpression of TNF-α did not appear to slow the resolution process and only increased the homeostatic population level of alveolar neutrophils, but the action of the signalling molecules was limited to generating the recruitment signal for neutrophils and not modulating the behavioural rules of the macrophage agents. On the other hand, Giles *et al.* (2001) [38] state that studies on the potential of TNF-α, TGF-β, GM-CSF and IL-1 to influence phagocytic clearance have demonstrated only limited effects and so adapting the efferocytosis model to allow these cytokines to modulate macrophage behaviour would be of questionable relevance.

I originally intended to include feedback loops in the production of signalling molecules. Figure 8 in Fadok *et al.* [32] shows that TGF-β added to cell culture led to increased production of TGF-β *in vitro.* and also inhibited production of TNF-α. A similar promotion/inhibition feedback mechanism may also be caused by increased extracellular levels of TNF-α.

With feedback loops influencing production of the two signalling molecules it is possible that modulation of cytokine expression would have a significant effect on the model outcome, provided suitable mechanisms existed to maintain constant high level of pro-inflammatory signalling. A further study of the available data on this factor combined with experimentation with a number

[9] Consultation with Carol Ogden

of potential feedback mechanisms would be a useful future project to shed light on the complex interactions of these two cytokines, as well as numerous others.

Other potential mechanisms which were neglected in this version of the model but could also be of interest for further study or resolution dynamics include allowing modulation of the collectin levels rather than setting them at a fixed value, including external influences on the rate of neutrophil apoptosis (such as acceleration by TNF-α ligation), a more detailed treatment of the neutrophil recruitment mechanism involving separate mechanisms for chemotactic attraction, tethering and extravasation and also a study of lipid-mediated resolution mechanisms either in tandem with, or instead of the cytokines used in this version.

6.1 Standards in agent-based and hybrid modelling

Mathematical and computer modelling are increasingly being used as tools to augment experimental biological research under the premise that a system can only be understood when its individual parts (defined in detail by traditional experimental methods) are 'plugged together' to form a whole.

Edmonds [39] reviews methods and applications of multi-agent based simulation (MABS), pointing out that simulation can be employed for a wide range of purposes (he cites entertainment, art, illustration of mathematical principles, an alternative to symbolic deduction for calculations relating to distributed systems, a medium for social exploration and a tool for scientific deductions).

He presents such simulations as a series of levels of abstraction built up from a physical theory describing the underlying, or target, system. Once a working model is sketched, he highlights practical steps by which the insight provided on the target system can be improved. This chiefly involves either increasing the rigour of the formal abstraction or, conversely, adding features to describe more richly the target system. Successful modelling, then, is the ability to optimise these two steps without losing insight: an overly rigourous abstraction becomes entirely theoretical with no relevance any real systems and adding too many layers of detail makes inference less concrete and the exact meaning of some components of the abstraction may become ambiguous.

Federici *et al.* [40] introduce a schema of four modelling stages built on a number of ideas raised in the Edmonds paper. These four layers describe both the building up of abstraction from the target system to a software implementation and also translating the output of the specific implementation of the simulation to any potential insights into or predictions about the target system (see Figure 18). Shifts in context and meaning must be considered at each stage of translation: scientists are used to declaring assumptions in construction of the conceptual model of a system, but translating a conceptual model into a computable program (stage 2 in the figure) may also require further abstraction (for example requiring events to be scheduled in a particular order rather than allowing them to happen simultaneously) and even implementing the computational model in a specific language (stage 3) may require further adjustment to comply with the constraints of the language. Given these caveats, the output data may only be interpreted in terms of the 'software' level and must undergo an analogous translation back down the levels (stages 6–9) if the developer is to be able to infer anything about the target system. Naturally, a clear documentation of the translation with distinct nomenclature for the entities in each stage is a crucial aid to maintaining the logical clarity during model development.

Stages 1–9 define a cyclical development process by which the interpretation of model output provides the

6.2 Conclusion

The experience of developing this model and reading of papers on similar subjects has highlighted a number of useful applications of agent-based modelling as well as a number of pitfalls which should be considered from the outset.

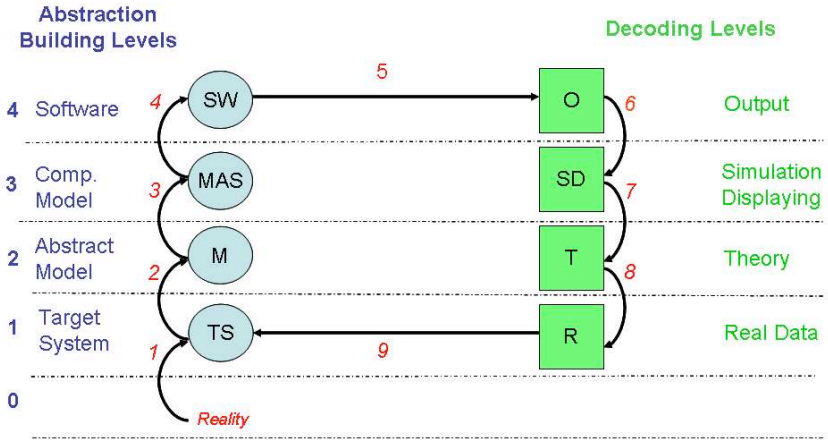

Figure 18: Layers of abstraction built on the target system in the schema by Federici *et al.* [40]

Firstly, even the early stages of model development require the modeller clearly to define the desired modes of behaviour, the routes by which agents interact and a number of parameters constraining the system. Even without seeking to model the system accurately, the process of conceptual planning provides a valuable service in creating a coded schema of the target system, highlighting those areas which are less understood. The process of planning a computational implementation also forces rigourous definition of entities and mechanisms, forcing the developer to consider possible ambiguities which may lie in descriptions using natural language.

To use ABMs more directly for scientific inference, the literature highlights two main approaches: one where the individual components and their interactions are assumed to be well-defined and the simulation simply plugs them together in order to predict properties of the system, and one where the systemic outcome is known but there exist a range of competing hypotheses for the component mechanisms and the modelling approach is to build a range of competing models and test these against the known outcome.

The first approach—essentially *in silico* empiricism—offers the advantage of exact control over parameter values and, in most cases at least, cheaper and quicker returns of data than an *in vitro* or *in vivo* experiment. In practise, the complexity of biological systems mean that there is likely to be a significant degree of uncertainty in the behaviour of the system components and hence the results inferred must also be taken in that context. The sensitivity of the global-level outcomes to parameter variation should be tested extensively and possible alternatives to behavioural rules considered. The hybrid model based on the *Epitheliome* project developed by Walker *et al.* [3] falls into this category of application and the authors are clear in the discussion about the large number of estimated parameters and the limitations in validity of the model output. They also feature an analysis of the sensitivity of cell receptor occupancy to variation of a large number of model parameters.

The use of ABM as a means to test competing hypotheses appears more scientifically rigourous. There is a clear definition of competing hypotheses and the output data should quantitatively demonstrate the strength of one hypothesis over the other. Of course, many of the above limitations also apply to this application since it is possible that changing parts of the model which are not under consideration would affect which hypothesis was rejected. The Warrender paper [4] uses ABM to test two hypotheses on maintenance of alveolar macrophage population numbers. Although neither hypothesis was definitively rejected, using the hypothesis test as a motivation for the model development provides a clear direction both in defining the conceptual system and in analysis of the output and the authors were able to identify a number of key processes in the

system and highlight areas where experimental data was lacking.

Both of the above authors noted that the models developed were limited in immediate application but provided a framework for development of future cell-signalling models. Further progress would be largely reliant on the availability of more specific data relating to individual cell characteristics.

It is difficult to define the efferocytosis model as a finished product representing either of these two approaches. With regard to the Federici *et al.* schema, it is at the stage of having cycled once through the abstraction and interpretation process before revision and re-implementation. In comparison with the Warrender paper, there was no clear set of conflicting mechanisms for apoptotic cell clearance which could be compared with one another and the data on cell signalling so scarce that the use of the model as an accurate predictive tool is extremely limited.

As with the two papers discussed above, much of the benefit of developing this model was highlighting areas which might potentially affect outcome: impedance of cell movement and low levels of pulmonary surfactants (collectins) were strongly implicated as defects which could lead to high residual populations of neutrophils in the alveolus.

The necessary adjustment of the physical dimensions of the model to allow for unrestricted cell movement highlighted the potential need to take the dynamical properties of cell movement and plasticity into account in future modelling attempts.

As with the Walker and Warrender models, the efferocytosis model represents a developmental snapshot with the potential to be extended in a number of different directions.

The most important requirement is further consultation with experimental researchers in order to validate the behaviours and parameters currently implemented, suggest revisions and, if possible, conduct *in vivo* or *in vitro* experiments to parameterise the model more accurately. At the current state of understanding of the system I think it would be most appropriate to apply the model in the hypothesis testing context, particularly testing potential mechanisms of cytokine inhibition and expression.

Another possible application is to develop the model as a demonstration or teaching tool, without aiming to reproduce the minutiae of system behaviour. This could serve as an interactive video illustration of the mechanisms involved in inflammatory resolution either for students or in a research context.

The two hybrid models discussed above and the efferocytosis model sought to describe the behaviour of a specific system but all have ended up at a similar 'half-way' point with the potential to be applied to other biological problems: a significant proportion of the modelling work in Walker's, Warrender's and my work could, with a little work, be applied to one of the other two systems. While this strengthens the argument for closer integration of the experimental and computational arms of research in order to develop biomedical models to an applicable level, it also suggests that a more useful approach for the theoretical side would be the development of generalised cell-signalling modelswhich could then be altered to fulfil the needs of a specific system as and when available data and behavioural observations become available.

Such a framework could, theoretically, concentrate on the common features of receptor-mediated cell signalling with generalised classes to handle the dynamics of receptor-ligand binding with the option of receptor internalisation, recycling etc. and then the behavioural rules could be defined by the modeller specific to the target system. This would reduce the time spent on coding shared properties of cell-signalling models, leaving more time to test and develop other aspects of the model. These possible paths for further development of the model are summarised in Figure 19.

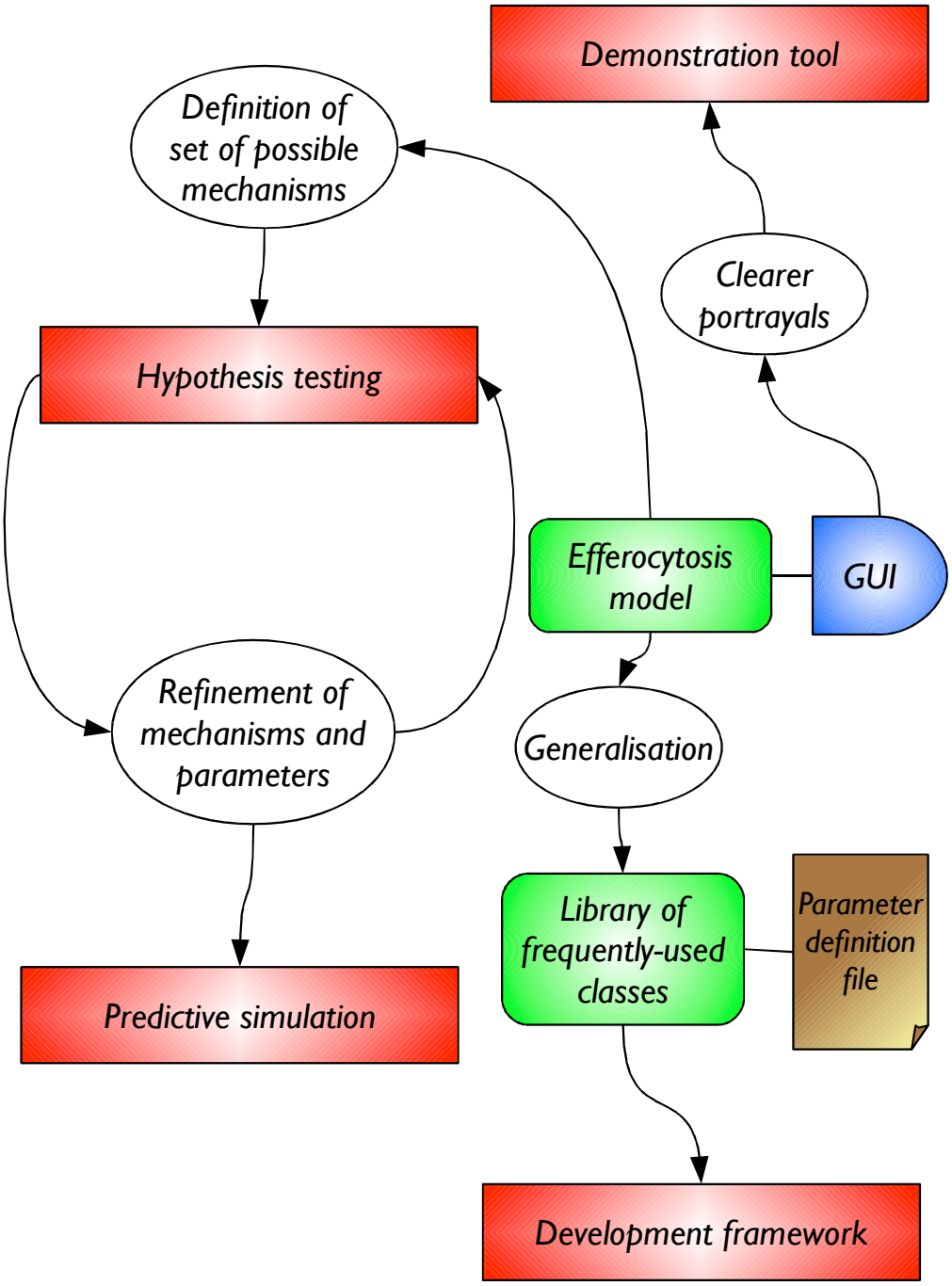

Figure 19: Possible ways in which the efferocytosis model could be further developed

A Mathematics

A.1 Chemotaxis

To achieve a simulation of chemoattraction, we set up a vector (X, Y) initialised to $(\cos\theta, \sin\theta)$, where θ is the current agent direction. Then we create an array of all objects within a specified distance and define:

$$X = \cos\theta + \sum_{array} \frac{\delta x_+}{\delta x_+^2 + \delta y_+^2} - \sum_{array} \frac{\delta x_-}{\delta x_-^2 + \delta y_-^2}$$

$$Y = \sin\theta + \sum_{array} \frac{\delta y_+}{\delta x_+^2 + \delta y_+^2} - \sum_{array} \frac{\delta y_-}{\delta x_-^2 + \delta y_-^2}$$

where δx and δy denote the difference in position between the phage and its surrounding objects and the subscripts denote an attraction (to opsonised or necrotic agents) or a repulsion (to other phages).

We then set the new direction of motion as $\arctan\left(\frac{Y}{X}\right)$.

A.2 Receptor occupation dynamics

For the receptors detecting presence of apoptotic or necrotic cells, if N denotes the total number of receptors of which R are occupied at any point in time and k_+ and k_- are association and dissociation rate constants we have:

$$\frac{\Delta R^{apop}}{\Delta t} = k_+^{apop} C^{apop} \left(1 - \frac{R^{apop}}{N^{apop}}\right) - k_-^{apop} \frac{R^{apop}}{N^{apop}}$$

$$\frac{\Delta R^{nec}}{\Delta t} = k_+^{nec} C^{nec} \left(1 - \frac{R^{nec}}{N^{nec}}\right) - k_-^{nec} \frac{R^{nec}}{N^{nec}}$$

Where superscripts respectively indicate constants and variables relating to the apoptotic or necrotic systems.

A similar pair of equations governs the number of complexes of TGF-β and TNF-α in each timestep:

$$\frac{\Delta R^{\beta}}{\Delta t} = k_+^{\beta} C^{\beta} \left(1 - \frac{R^{\beta}}{N^{\beta}}\right) - k_-^{\beta} \frac{R^{\beta}}{N^{\beta}}$$

$$\frac{\Delta R^{\alpha}}{\Delta t} = k_+^{\alpha} C^{\alpha} \left(1 - \frac{R^{\alpha}}{N^{\alpha}}\right) - k_-^{\alpha} \frac{R^{\alpha}}{N^{\alpha}}$$

A.3 Cytokine production

The production of cytokines is implemented with a linear combination of the proportion of occupied receptors $\frac{R^{apop}}{N^{apop}}$ and $\frac{R^{nec}}{N^{nec}}$:

$$P^{\beta} = P_{max}^{\beta} k_{hom}^{\beta} \left(1 + \left(\frac{1 - k_{hom}^{\beta}}{k_{hom}^{\beta}}\right) \frac{R^{apop}}{N^{apop}} - \frac{R^{nec}}{N^{nec}}\right)$$

$$P^{\alpha} = P_{max}^{\alpha} k_{hom}^{\alpha} \left(1 + \left(\frac{1 - k_{hom}^{\alpha}}{k_{hom}^{\alpha}}\right) \frac{R^{nec}}{N^{nec}} - \frac{R^{apop}}{N^{apop}}\right)$$

Where k_{hom} denotes a 'homeostatic' production signal when there is no stimulus and P_{max} denotes the maximum rate of production when all receptors are occupied. The rate of production with no stimulus is $k_{hom} P_{max}$.

A.4 Changes in background concentration

The concentrations C^α and C^β in the surrounding medium then vary over time according to:

$$\frac{\Delta C^\beta}{\Delta t} = Q^\beta \left(P^\beta + k_-^\beta \frac{R^\beta}{N^\beta} - k_+^\beta C^\beta \left(1 - \frac{R^\beta}{N^\beta} \right) - k_{deg}^\beta C^\beta \right)$$

$$\frac{\Delta C^\alpha}{\Delta t} = Q^\alpha \left(P^\alpha + k_-^\alpha \frac{R^\alpha}{N^\alpha} - k_+^\alpha C^\alpha \left(1 - \frac{R^\alpha}{N^\alpha} \right) - k_{deg}^\alpha C^\alpha \right)$$

Here k_{deg} is a degradation rate constant, representing the rate at which signalling molecules disperse, decompose or are recycled by cells in the environment and Q is a 'molarity conversion constant' allowing us to convert between numbers of molecules being produced or decomposed into the concentrations in the surrounding medium.

A.5 Parameter values

Unless otherwise indicated, simulations were run with variables/constants initialised at the following values:

Variable/constant	Value
k_+^{apop}	0.05
k_-^{dpop}	0.5
k_+^{nec}	0.05
k_-^{nec}	0.5
k_+^β	0.00185
k_-^β	0.5
k_+^α	0.00278
k_-^α	0.5
k_{hom}^β	0.333
k_{hom}^α	0.0909
P_{max}^β	0.135
P_{max}^α	0.33

Variable/constant	Value
N^{apop}	100
N^{nec}	100
N^β	100
N^α	100
R^{apop}	0
R^{nec}	0
R^β	10
R^α	10
C^β	30
C^α	20
Q^β	1
Q^α	1
k_{deg}^β	0.0015
k_{deg}^α	0.0015

B Graphs of output

B.1 Neutrophil numbers

Timecourses of average neutrophil population size over 20 simulations. Parameter varied from minimum (purple) to maximum (red) value. See Table 3 for values.

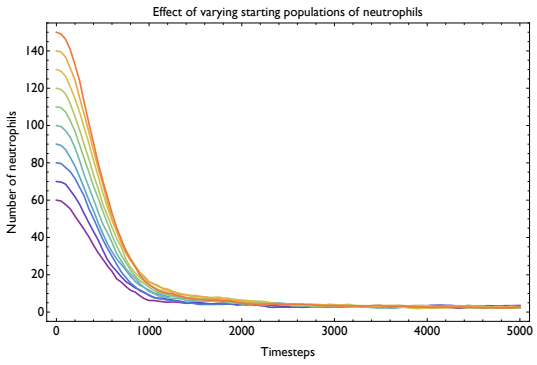

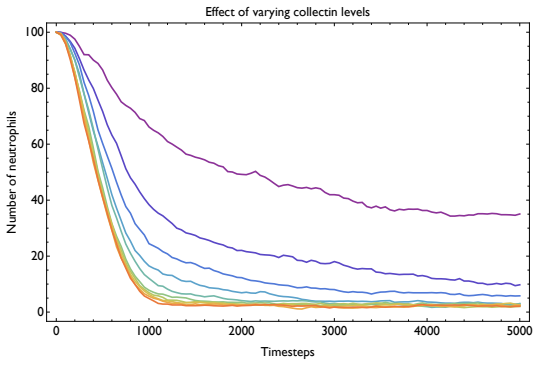

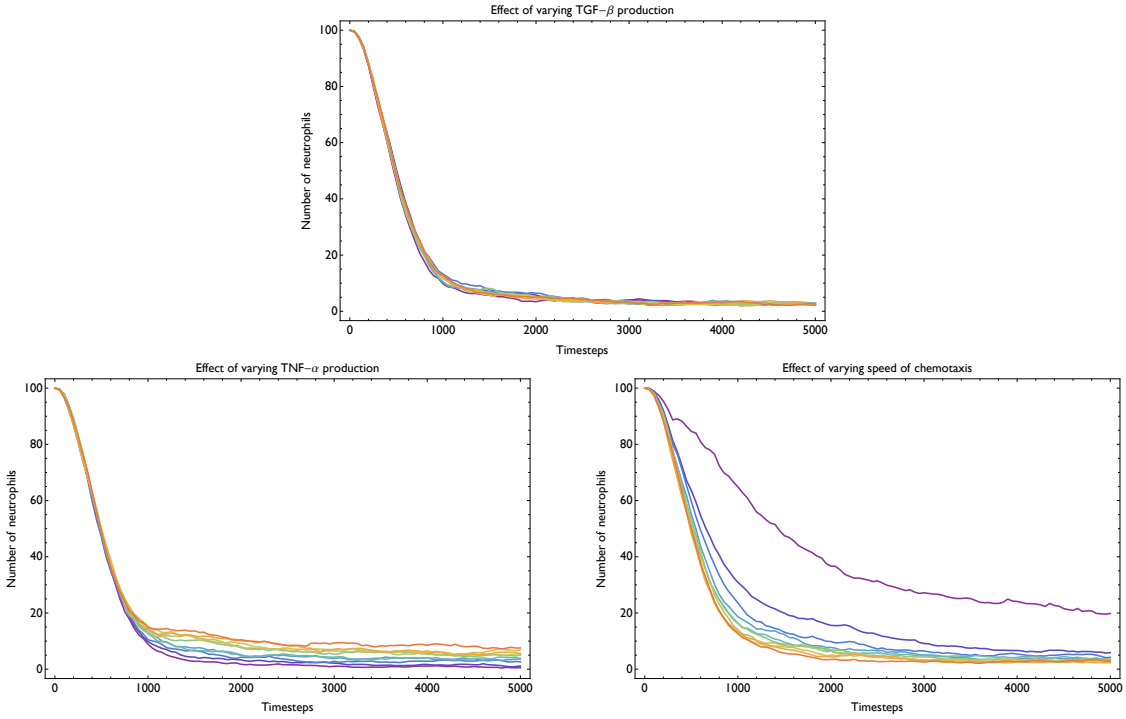

B.2 Neutrophil recruitment

Timecourses of average `neutroProb` value over 20 simulations. Parameter varied from minimum (purple) to maximum (red) value. See Table 3 for values.

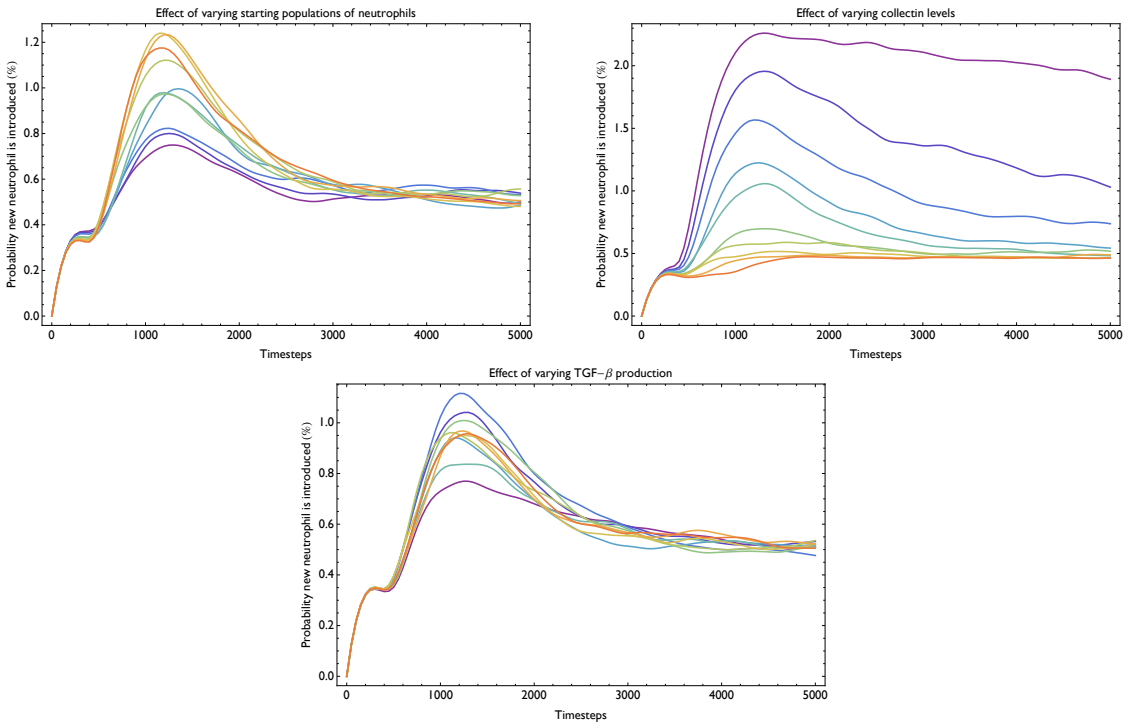

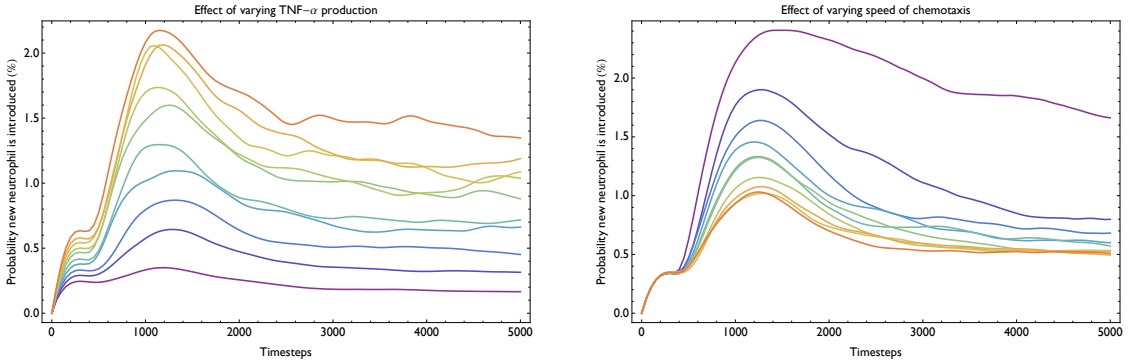

B.3 TGF-β concentrations

Timecourses of average TGF-β concentration over 20 simulations. Parameter varied from minimum (purple) to maximum (red) value. See Table 3 for values.

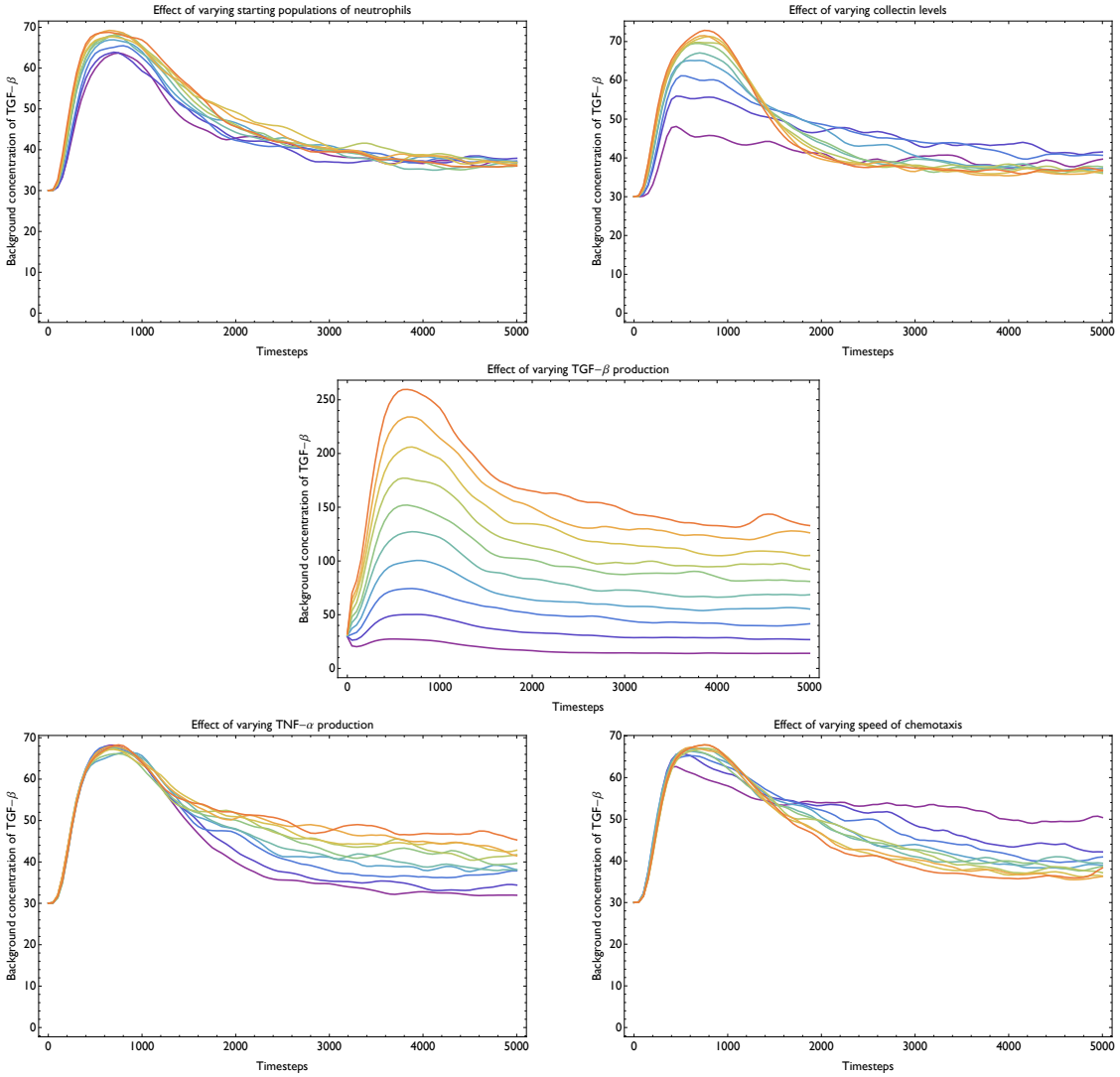

B.4 TNF-α concentrations

Timecourses of average TNF-α concentration over 20 simulations. Parameter varied from minimum (purple) to maximum (red) value. See Table 3 for values.

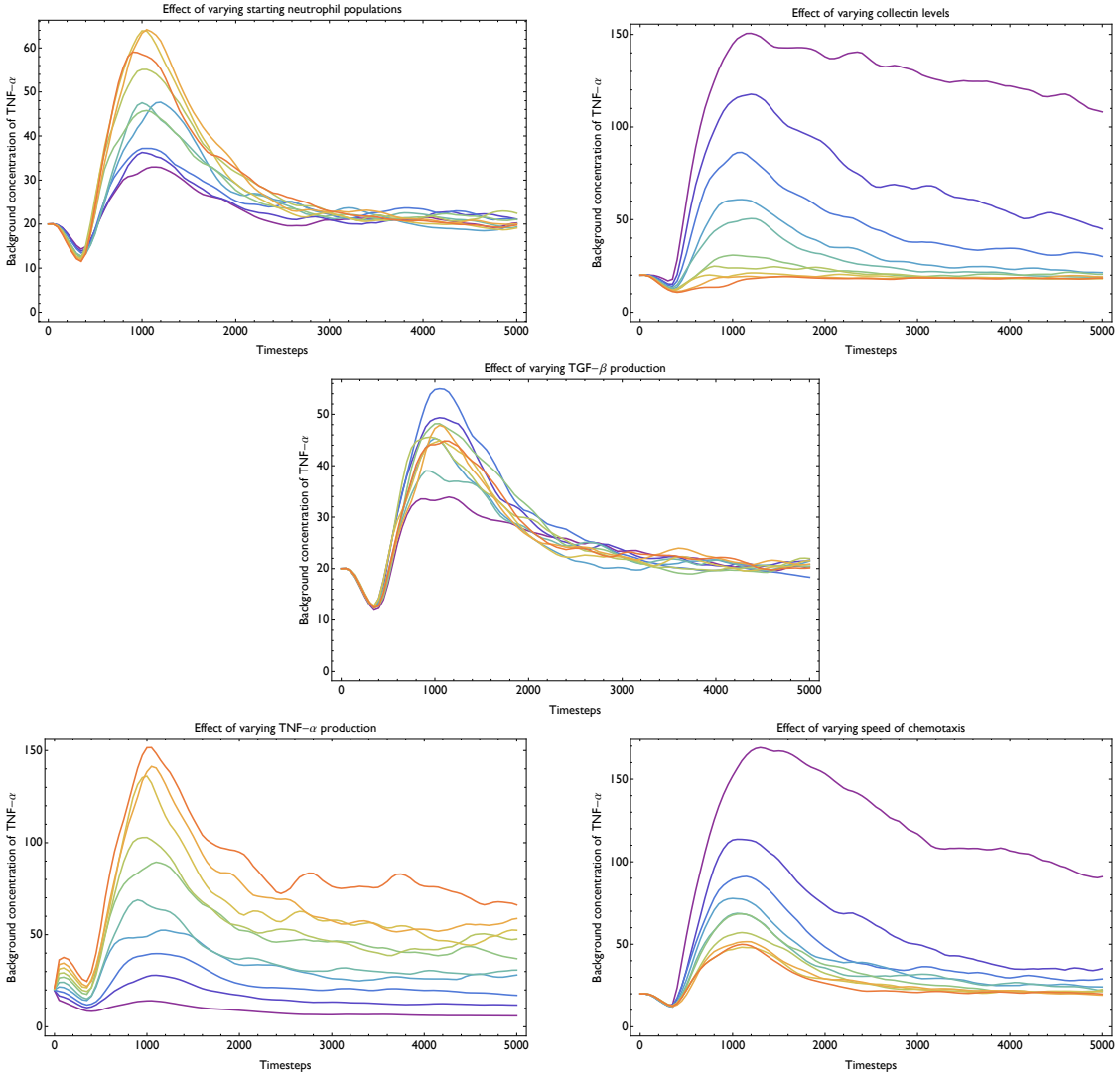

C Mathematica code

C.1 Population dynamics sketch model

The code and output graphs for the Mathematica sketch model. Interestingly, there was an abrupt change in behaviour as the number was increased from 20 to 21. With 20 or fewer macrophages the number of necrotic cells increases to a maximum, whereas at 21 it is uniformly zero.

```
MaxNeutro = 1000;
MaxBR = 50;
Macro = 19;
NecContrib = 5;
EatContrib = 1;
EatRate = 0.5;
NTimeStep = 100;

Live = {10, 10, 10, 10, 10, 10, 10, 10, 10, 10};
Apop = {0, 0};
```

```
Nec = 0;
Inflam = 0.5;
Neutro = Sum[Live[[i]], {i, 1, 10}];
Birth = Floor[MaxBR*Inflam*Log[2 - (Neutro/MaxNeutro)]/Log[2]];
Eat = 0;

LiveChart = {Sum[Live[[i]], {i, 1, 10}]};
ApopChart = {Sum[Apop[[i]], {i, 1, 2}]};
NecChart = {Nec};

For[i = 1, i <= NTimeStep, i++,
 Nec += Apop[[2]];
 Apop[[2]] = Apop[[1]];
 Apop[[1]] = Live[[10]];
 LiveTemp = Table[Live[[i]], {i, 1, 9}];
 Live = Join[{Birth}, LiveTemp];
 Edible = Apop[[1]] + Apop[[2]] + Nec;
 If[Edible != 0,
  EatApop1 = Floor[EatRate*Macro*(1 - Exp[-Apop[[1]]])*Apop[[1]]/Edible];
  EatApop2 = Floor[EatRate*Macro*(1 - Exp[-Apop[[2]]])*Apop[[2]]/Edible];
  EatNec = Floor[EatRate*Macro*(1 - Exp[-Nec])*Nec/Edible];
  Eat = EatApop1 + EatApop2 + EatNec;
  Nec = Max[Nec - EatNec, 0];
  Apop[[1]] = Max[Apop[[1]] - EatApop1, 0];
  Apop[[2]] = Max[Apop[[2]] - EatApop2, 0];
  Inflam =
   Max[Inflam + (NecContrib*Apop[[2]] - EatContrib*Eat)/(NecContrib*Apop[[2]]
   + EatContrib*Eat), 0]];
 Neutro = Sum[Live[[i]], {i, 1, 10}] + Sum[Apop[[i]], {i, 1, 2}] + Nec;
 Birth = Max[Floor[MaxBR*Inflam*Log[2 - (Neutro/MaxNeutro)]/Log[2]],0];
 AppendTo[LiveChart, Sum[Live[[i]], {i, 1, 10}]];
 AppendTo[ApopChart, Sum[Apop[[i]], {i, 1, 2}]];
 AppendTo[NecChart, Nec] ]
```

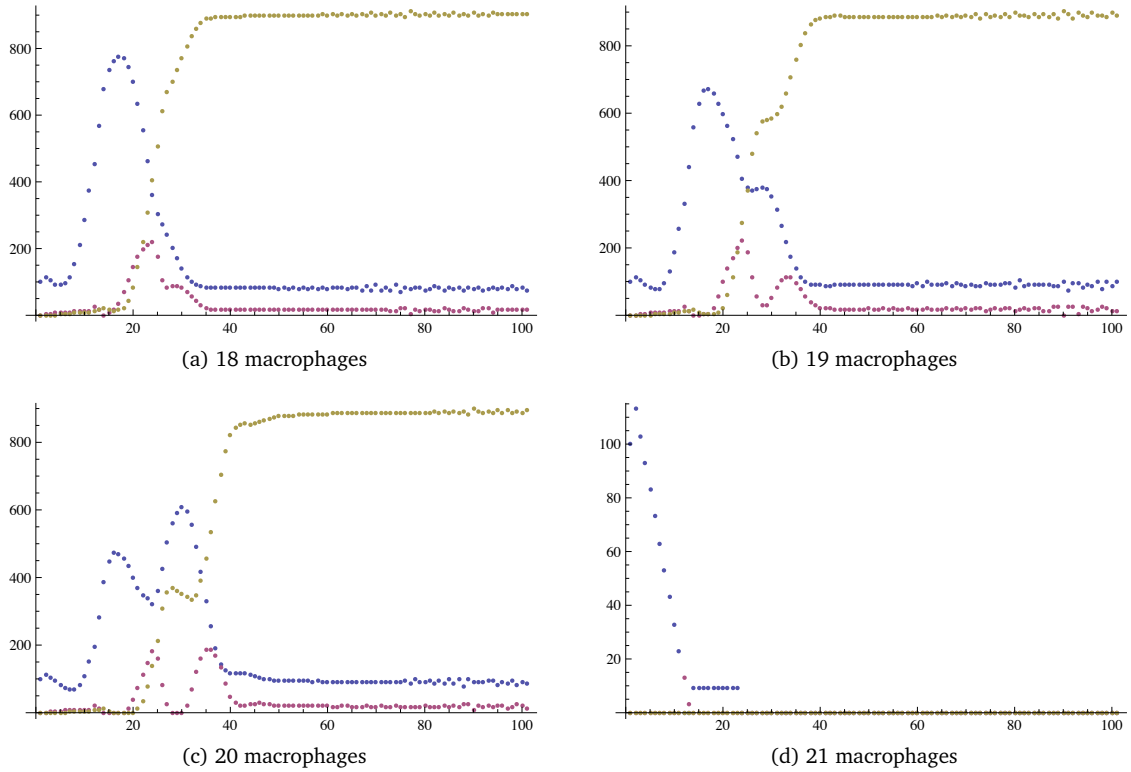

(a) 18 macrophages

(b) 19 macrophages

(c) 20 macrophages

(d) 21 macrophages

Figure 20: Population dynamics of live (blue), apoptotic (purple) and necrotic (yellow) neutrophils over 100 timesteps

C.2 Receptor dynamics sketch

```
Macrophage signalling model
f1[RApop_] :=
 RApop + kApop1*CApop*(1 - (RApop/NApop)) - kApop2*(RApop/NApop)
g1[RNec_] := RNec + kNec1*CNec*(1 - (RNec/NNec)) - kNec2*(RNec/NNec)
f2[RBeta_] :=
 RBeta + kBeta1*CBeta*(1 - (RBeta/NBeta)) - kBeta2*(RBeta/NBeta) -
  kBetaInt*(RBeta/NBeta)
g2[RAlpha_] :=
 RAlpha + kAlpha1*CAlpha*(1 - (RAlpha/NAlpha)) -
  kAlpha2*(RAlpha/NAlpha) - kAlphaInt*(RAlpha/NAlpha)
FBeta[IBeta_, IAlpha_] :=
 kHomBeta (1 + ((1 - kHomBeta)/kHomBeta)*(RApop/NApop)*
     IBeta - (RNec/NNec)*IAlpha)
FAlpha[IBeta_, IAlpha_] :=
 kHomAlpha (1 + ((1 - kHomAlpha)/kHomAlpha)*(RNec/NNec)*
     IAlpha - (RApop/NApop)*IBeta)
PBeta[IBeta_, IAlpha_] :=
 FBeta[IBeta, IAlpha]*(PBetaMax/FBetaHalf + FBeta[IBeta, IAlpha])
PAlpha[IBeta_, IAlpha_] :=
 FAlpha[IBeta, IAlpha]*(PAlphaMax/FAlphaHalf + FAlpha[IBeta, IAlpha])
f3[CBeta_] :=
 CBeta + (PBeta[IBeta, IAlpha] + kBeta2*(RBeta/NBeta) -
     kBeta1*CBeta*(1 - (RBeta/NBeta)))*QBeta
g3[CAlpha_] :=
 CAlpha + (PAlpha[IBeta, IAlpha] + kAlpha2*(RAlpha/NAlpha) -
     kAlpha1*CAlpha*(1 - (RAlpha/NAlpha)))*QAlpha
kApop1 =
  0.4;   (*Association, dissociation, internalisation rate constants*)

kApop2 = 0.4;
kNec1 = 0.7;
kNec2 = 0.3;
kBeta1 = 0.2;
kBeta2 = 0.2;
kBetaInt = 0.01;
kAlpha1 = 0.6;
kAlpha2 = 0.1;
kAlphaInt = 0.03;
kHomBeta = 0.01;   (*Homeostatic output of F ie. F(0,0) = kHom *)

kHomAlpha = 0.01;
CApop = 0.4;     (*Initial background concentrations*)
CNec = 0.6;
CBeta = 0.6;
CAlpha = 4.2;

NApop = 100;   (*Numbers of receptors*)
NNec = 100;
NBeta = 100;
NAlpha = 100;
RApop = 50;   (*Initial number of receptors occupied*)
RNec = 50;
RBeta = 50;
RAlpha = 50;

PAlphaMax = 1;  (*Maximum production of signalling molecules/timestep*)
PBetaMax = 1;
FBetaHalf = 0.5;  (*Input value giving an output of half PMax*)
FAlphaHalf = 0.5;

QBeta = 0.1;     (*"Molar" conversion constant*)
QAlpha = 0.1;
RApopTab = {};  (*Tables for storing values at each timestep*)

RNecTab = {};
RBetaTab = {};
RAlphaTab = {};
PAlphaTab = {};
PBetaTab = {};
```

```
CBetaTab = {};
CAlphaTab = {};
For[i = 0, i < 2000, i++,
 RApop = f1[RApop];
 RNec = g1[RNec];
 AppendTo[RApopTab, RApop];
 AppendTo[RNecTab, RNec];
 RBeta = f2[RBeta];
 RAlpha = g2[RAlpha];
 AppendTo[RBetaTab, RBeta];
 AppendTo[RAlphaTab, RAlpha];
 IBeta = kBetaInt*(RBeta/NBeta);
 IAlpha = kAlphaInt*(RAlpha/NAlpha);
 AppendTo[PBetaTab, PBeta[IBeta, IAlpha]];
 AppendTo[PAlphaTab, PAlpha[IBeta, IAlpha]];
 CBeta = f3[CBeta];
 CAlpha = g3[CAlpha];
 AppendTo[CBetaTab, CBeta];
 AppendTo[CAlphaTab, CAlpha];
 CNec *= 0.9;
 ]
CAlpha
0.946958
ListPlot[{RApopTab, RNecTab},
 PlotLabel -> "Number of occupied receptors: apoptotic vs. necrotic"]
ListPlot[{RBetaTab, RAlphaTab},
 PlotLabel -> "Number of occupied receptors: TGF-beta vs. TNF-alpha"]
ListPlot[{PBetaTab, PAlphaTab},
 PlotLabel -> "Expression of TGF-beta/TNF-alpha over time"]
ListPlot[{CBetaTab, CAlphaTab},
 PlotLabel ->
  "Background concentration of TGF-beta/TNF-alpha over time"]
```

References & resources

[1] Volker Grimm, Eloy Revilla, Uta Berger, Florian Jeltsch, Wolf M. Mooij, Steven F. Railsback, Hans-Hermann Thulke, Jacob Weiner, Thorsten Wiegand, and Donald L. DeAngelis. Pattern-oriented modeling of agent-based complex systems: lessons from ecology. *Science*, 310:987–991, 2005.

[2] S.F. Railsback. Getting "results": the pattern-oriented approach to analyzing natural systems with individual-based models. *Natural Resource Modelling*, 14(3):465–475, 2001.

[3] Dawn Walker, Steven Wood, Jennifer Southgate, Mike Holcombe, and Rodney Smallwood. An integrated agent-mathematical model of the effect of intercellular signalling via the epidermal growth factor receptor on cell proliferation. *J. Theor. Biol.*, 242, 2006.

[4] Christina Warrender, Stephanie Forrest, and Lee Segel. Homeostasis of peripheral immune effectors. *Bull. Math. Biol.*, 66(6):1493–1514, 2004.

[5] Christina Elizabeth Warrender. *Modeling intercellular interactions in the peripheral immune system*. PhD thesis, University of New Mexico, 2004.

[6] William A. Griffin. Agent-based modeling for the theoretical biologist. *Biological theory*, 1(4):404–409, 2006.

[7] Mark A. Bedau. Can unrealistic computer models illuminate theoretical biology? In Annie S. Wu, editor, *Genetic and Evolutionary Computation Conference Workshop Program*, pages 20–23, 1999.

[8] Bryan C. Thorne. Combining experiments with multi-cell agent-based modeling to study biological tissue patterning. *Briefings in Bioinformatics*, 2007.

[9] Peter M. Henson. Dampening inflammation. *Nature Immunology*, 6:1179–1181, 2005.

[10] Charles N. Serhan. A search for endogenous mechanisms of anti-inflammation uncovers novel chemical mediators: missing links to resolution. *Histochem. Cell Biol.*, 122:305–321, 2004.

[11] Charles N. Serhan and John Savill. Resolution of inflammation: the beginning programs the end. *Nature Immunology*, 6(12):1191–1197, 2005.

[12] Thomas J. Kindt, Richard A. Goldsby, and Barbara A. Osborne. *Kuby Immunology, Sixth Edition*. W.H. Freeman and Company, 2007.

[13] Lauren Sompayrac. *How the Immune System Works, 2nd Edition*. Blackwell Publishing, 2003.

[14] Bart N. Lambrecht. Alveolar macrophage in the driver's seat. *Immunity*, 24:366–367, 2006.

[15] Christopher Haslett. Granulocyte apoptosis and its role in the resolution and control of lung inflammation. *Am. J. Respir. Crit. Care Med.*, 160:S5–S11, 1999.

[16] Peter M. Henson, Donna L. Breaton, and Valerie A. Fadok. The phosphatidylserine receptor: a crucial molecular switch? *Nat. Rev. Mol. Cell Biol.*, 2:627–633, 2001.

[17] Ben B. Whitlock, Shyra Gardai, Valerie Fadok, Donna Bratton, and Peter M. Henson. Differential roles for $\alpha_m\beta_2$ integrin clustering or activation in the control of apoptosis via regulation of Akt and ERK survival mechanisms. *J. Cell Biol.*, 151(6):1305–1320, 2000.

[18] Wei Xu, Anja Roos, Mohamed R. Daha, and Cees van Kooten. Dendritic cell and macrophage subsets in the handling of dying cells. *Immunobiology*, 211:567–575, 2006.

[19] Peter M. Henson, Donna L. Bratton, and Valerie A. Fadok. Apoptotic cell removal. *Curr. Biol.*, 11:R795–R805, 2001.

[20] R. William Vandivier, Peter M. Henson, and Ivor S. Douglas. Burying the Dead. *Chest*, 129:1673–1682, 2006.

[21] Peter M. Henson, Gregory P. Cosgrove, and R. William Vandivier. Apoptosis and cell homeostasis in chronic obstructive pulmonary disease. *Proc. Am. Thorac. Soc.*, 3:512–518, 2006.

[22] Shyra J. Gardai, Kathleen A. McPhillips, S. Courtney Frasch, William J. Janssen, Anna Starefeldt, Joanne E. Murphy-Ullrich, Donna L. Bratton, Per-Arne Oldenborg, Marek Michalak, and Peter M. Henson. Cell-surface calreticulin initiates clearance of viable of apoptotic cells through *trans*-activation of LRP on the phagocyte. *Cell*, 123:321–334, 2005.

[23] R. William Vandivier, Carol Anne Ogden, Valerie A. Fadok, Peter R. Hoffmann, Kevin K. Brown, Marina Botto, Mark J. Walport, James H. Fisher, Peter M. Henson, and Kelly E. Greene. Role of surfactant proteins A,D, and C1q in the clearance of apoptotic cells in vivo and in vitro: Calreticulin and CD91 as a common collectin receptor complex. *J. Immunol.*, pages 3978–3986, 2002.

[24] Howard Clark, Nades Palaniyar, Samuel Hawgood, and Kenneth B.M. Reid. A recombinant fragment of human surfactant protein D reduces alveolar macrophage apoptosis and pro-inflammatory cytokines in mice developing pulmonary emphysema. *Ann. N. Y. Acad. Sci.*, 1010:113–116, 2003.

[25] Nades Palanyiar, Howard Clark, Jeya Nadesalingam, Michael J. Shih, Samuel Hawgood, and Kenneth B.M. Reid. Innate immune collectin surfactant protein D enhances the clearance of DNA by macrophages and minimizes anti-DNA antibody generation. *J. Immunol.*, pages 7352–7358, 2005.

[26] John F. Alcorn and Jo Rae Wright. Surfactanct protein A inhibits alveolar macrophage cytokine production by CD14-independent pathway. *Am. J. Physiol. Lung Cell Mol. Physiol.*, 286:L129–L136, 2004.

[27] Shyra J. Gardai, Yi-Qun Xiao, Matthew Dickinson, Jerry A. Nick, Dennis R Voelker, Kelly E. Greene, and Peter M. Henson. By binding SIRPα or calreticulin/CD91, lung collectins act as dual function surveillance molecules to suppress or enhance inflammation. *Cell*, 115:13–23, 2003.

[28] Dror Mevorach, John O. Mascarenhas, Debra Gershov, and Keith B. Elkon. Complement-dependent clearance of apoptotic cells by human macrophages. *J. Exp. Med.*, 188(12):2313–2320, 1998.

[29] Shyra J. Gardai, Donna L. Bratton, Carol Anne Ogden, and Peter M. Henson. Recognition ligands on apoptotic cells: a perspective. *Journal of Leukocyte Biology*, 79:896–903, 2006.

[30] Jiahuai Han and Richard J. Ulevitch. Limiting inflammatory responses during activation of innate immunity. *Nature Immunology*, 6(12):1198–1205, 2005.

[31] Rona S. Scott, Eileen J. McMahon, Shannon M. Pop, Elizabeth A. Reap, Roberto Caricchio, Philip L. Cohen, H. Shelton Earp, and Glenn K. Matsushima. Phagocytosis and clearance of apoptotic cells is mediated by MER. *Nature*, 411:207–211, 2001.

[32] Valerie A. Fadok, Donna L. Bratton, Anatole Konowal, Peter W. Freed, Jay Y. Westcott, and Peter M. Henson. Macrophages that have ingested apoptotic cells in vitro inhibit proinflamatory cytokine production through autocrine/paracrine mechanisms involving TGF-β, PGE2, and PAF. *J. Clin. Invest.*, 101(4):890–898, 1998.

[33] Gerard Cox. IL-10 enhances resolution of pulmonary inflammation in vivo by promoting apoptosis of neutrophils. *Am. J. Physiol.*, 271(15):L566–L571, 1996.

[34] Kenji Takabayashi, Maripat Corr, Tomoko Hayashi, Vanessa Redecke, Lucinda Beck, Donald Guiney, Dean Sheppard, and Eyal Raz. Induction of a homeostatic circuit in lung tissue by microbial compounds. *Immunity*, 24:475–487, 2006.

[35] Mark L. Lupher Jr. and W. Michael Gallatin. Regulation of fibrosis by the immune system. *Advances in immunology*, 89:245–288, 2006.

[36] Andrew D. Luster, Ronen Alon, and Ulrich H von Andrian. Immune cell migration in inflammation: present and future therapeutic targets. *Nat. Immunol.*, 6(12):1182–1190, 2005.

[37] Lee E. Limbird. *Cell surface receptors: a short course on theory and methods, Second Edition*. Kluwer Academic Publishers, 1996.

[38] Katherine M. Giles, Katherine Ross, Adriano G. Rossi, Neil A. Hotchin, Christopher Haslett, and Ian Dransfield. Glucocorticoid augmentation of macrophage capacity for phagocytosis of apoptotic cells is associated with reduced p130Cas expression, loss of Paxillin/pyk2 phosphorylation and high levels of active Rac. *J. Immunol.*, 167:976–986, 2001.

[39] B. Edmonds. The use of models—making MABS more informative. In S. Moss and P. Davidson, editors, *Multi-Agent-Based Simulation: Second Interntational Workshop*, 2000.

[40] Mizar Luca Federici, Stefano Redaelli, and Giuseppe Vizzari. Models, abstractions and phases in multi-agent based simulation. Manuscript.